DRAFT

THE USE OF MODELS TO UNDERSTAND THE AQUEOUS CHEMISTRY OF URANIUM

Pierre Vitorge,[1,2] Bertrand Siboulet,[3] Colin J. Marsden,[4] Thomas Vercouter[1]

[1]CEA, DEN, Saclay, Laboratoire de Spéciation des Radionucléides et Molécules, Gif-sur-Yvette, France.

[2]Université d'Evry, CEA, CNRS, Laboratoire Analyse et Modélisation pour la Biologie et l'Environnement, Evry, France.

[3]CEA, DEN, Marcoule, Laboratoire de conception des architectures moléculaires,Bagnols-sur-Cèze, France.

[4]Université P. Sabatier, CNRS, Laboratoire de Chimie et Physique Quantiques,Toulouse, France.

1. ABSTRACT

Uranium chemistry has been extensively studied in industrial (typically for the reprocessing of nuclear fuels) or environmental (typically for waste or pollution management) waters. Most of the aqueous reactions are sufficiently fast that modelling and predictions, derived from thermodynamics based on Gibbs energies of reaction ($\Delta_r G$) or equivalently from equilibrium constants of complexation and hydrolysis, solubility products and standard redox potentials, should be reliable. Measured $\Delta_r G$ values are usually converted into Gibbs energies of formation ($\Delta_f G$) in thermochemical data bases, using auxiliary data. We discuss briefly how and where to obtain and use these ($\Delta_r G$ and $\Delta_f G$) values, and the corresponding thermodynamic basis as developed for solution chemistry – including solid solutions. We show that correlations between these numerical values or with physical parameters give a comprehensive view of chemical reactivity, which can be used for better qualitative understanding and tentative predictions. The geometries of the chemical species are useful for this purpose, but it is difficult to obtain experimental geometries in solution. We emphasize that these geometries can now be obtained by molecular modelling, even though molecular modelling in aqueous solutions is more difficult than in the gas or solid phases. Several recent studies in which the hydration of actinide ions has been modelled by quantum chemistry, and by classical and quantum molecular modelling, are described. These studies enable us to explain trends in physical and chemical properties across the actinide series, including the anomalous properties of Pa: other classical analogies and rules of thumb help us to understand and tentatively predict the chemical behaviour of uranium and its chemical analogues.

2. INTRODUCTION

The aqueous chemistry of most inorganic species can be described with the equilibrium constants of the law of mass action, since their hydrolysis and complexation reactions are sufficiently fast to be observed in equilibrium conditions with aqueous inorganic –and even many small organic ligands. Such approach is currently used in all the scientific and technologic fields where solution chemistry is important. The aqueous chemistry of uranium is typically studied for industry (reprocessing of nuclear fuels based on liquid-liquid extraction), geochemistry (mining, depositories of wastes), biology (toxicity) and other applications. In these frameworks, solution chemists are required to identify the stoichiometries and measure the formation (equilibrium) constants of the relevant aqueous hydroxides and complexes of uranium in its relevant oxidation states: equilibrium constants are required for most of the macroscopic models, where chemistry is involved.

Equilibrium constant, K, is equivalent to $\Delta_r G$ (= -R T ln(K)), the Gibb's energy of the corresponding reaction: the law of mass action has been demonstrated -not discovered- from classical equilibrium thermodynamics. Classical thermodynamics tells that the equilibrium concentrations of all the aqueous species ("speciation") can be calculated from mass balances and thermodynamic data ($\Delta_r G$) at given pressure (P) and temperature (T). $\Delta_r G$ data typically give the quantitative reactivities of the ligands for the uranium ions in liquid waters; but thermodynamics does not specially give any qualitative explanation of the reactivities, since the $\Delta_r G$ data need to be measured. For this, chemists consider the geometries of the complexes and hydroxides, and they use qualitative concepts as typically hardness, covalent or ionic character of bonding, hydrogen bonding. These qualitative interpretations can be checked and further understood with molecular modelling.

Chemistry has recently been studied with molecular models based on quantum or parameterized classical mechanics. Such models usually provide the geometries and the energies of the chemical species; from which the energies of reactions are readily calculated; but most $\Delta_r G$ values are still measured, not obtained from molecular modelling of aqueous chemistry. Accurate energy calculations are certainly not the most straightforward use of molecular modelling in liquid water, while quantum calculations and molecular dynamics can provide other useful qualitative and quantitative pieces of chemical information. Up to now molecular modelling have been used to describe -or simulate- the hydration of uranium in the oxidation state six (U(VI)) in liquid water, and a few of its hydrolysed species and complexes, essentially aiming at validating molecular modelling approaches

In this chapter, we first describe the aqueous chemistry of uranium (Section 3) starting with the description of the aquo ion of uranium -and analogous actinides- (Section 3.1) and usual qualitative explanation of their stabilities and reactivities as typically their hard characters and the analogy between the f-block elements in the same oxidation state (Section 3.1.1). The standard potentials of their redox couples (Section 3.1.2) quantitatively give their relative stabilities at pH = 0 (Figure 1). In non complexing media these relative stabilities can be modified essentially by hydrolysis (Section 3.2) as

illustrated by the Pourbaix diagram of uranium that gives the (E,pH) domains of the predominating uranium ions and their hydrolysed species (Figure 2 a), while several minor species are also formed in equilibrium conditions (Figure 3). As expected it is easier to hydrolyse the uranium ions with the highest charge. Virtually the same trend is usually observed for complexation (Section 3.3). Consistently with their hard character, the actinide ions are believed to form stronger complexes with anionic ligand of more negative [charge / (ionic radius)] ratios. This is illustrated by an empirical correlation (Section 3.3.1) between the formation constant of 1-1 complexes and the acidity constants of the ligands (Figure 4). Among usual ligands in ground-waters (Section 3.3.4) CO_3^{2-} (Section 3.3.2) and SO_4^{2-} (Section 3.3.3) form strong and weak 1-1 bidentate complexes with the actinide ions. For a given ligand the strength of such complexes usually slightly increases with the atomic number across each f-block element series as a result of the decreasing of the ionic radius. For the same reason, the reverse trend can be observed for limiting complexes (Figure 6) as a result of steric repulsions (Figure 5). In this section (3) on experimental uranium aqueous chemistry we finally outline a few aspects of the thermodynamics as used by solution chemists (Section 3.4), first the thermodynamic data (Section 3.4.1) since among published formation constants (Section 3.4.1.1) inconsistencies exist: rather than compilations of all the published data, it is better to use a consistent -and critical- thermo-chemical data base, where data are missing for unresolved problems, and to estimate these missing data (Section 3.4.1.2). The practical definition of the standard state usually require activity coefficients (Section 3.4.1.3), which are often calculated with empirical parameters (Figure 7). Besides their obvious use to describe uranium aqueous chemistry, these thermodynamic data also give a synthetic picture to be compared with molecular modelling results. Thermodynamics as scientific base for solution chemistry also provide rigorous chemical concepts for other scientific fields. We here insists -essentially in footnotes- on the way of considering energies of reactions as applications of the law of mass action, especially half-reaction points. This also gives classical Pourbaix diagrams (Figure 2) and similar diagrams typically with the influence of complexing anions (Figure 2) or in the gas phase to display ab initio energy results (Figure 9). The law of mass action can also be used for solid solutions (Section 3.4.2) encompassing ionic exchange equilibria (Section 3.4.2.1), complicated mixture solid phases studied by geochemists, and even $U_{1-x}Np_xO_2$ (Section 3.4.2.2) and UO_{2+y} (Section 3.4.2.3). In this later case the theoretical redox potential curve as a function of y (Figure 9) has the same shape as experimental high temperature P_{O_2} curves.

After the description of uranium aqueous chemistry (Section 3), we select recent molecular modelling studies of uranium (Section 4). Our aim (Section 4.1) is not to give a comprehensive view of what could be done, or has been done, neither to explain the theory; we rather consider molecular modelling as existing tools for solution chemists. We give examples on the ways of using these tools, since studying ions in liquid water is not the most straightforward application of molecular modelling, especially for the main applications solution chemists are interested in (Section 3): elucidating the stoichiometries and relative stabilities -within less than 1 $kJ.mol^{-1}$- of the numerous

aqueous species (Figure 3) that are formed in given equilibrium conditions. For simplicity (Section 4.1) we focus on the U(VI) uranyl ion. We start with quantum calculations for geometry optimization of UO_2^{2+} progressively hydrated by adding H_2O molecules one by one, hence in the gas phase, and further hydrolysed by suppressing H^+ from a water molecule of the first hydration layer (Section 4.2). The energetic data are presented in the form of predominance diagrams. Such (DFT) quantum calculations are classically validated by comparing with mass spectrometry measurements (Section 4.3). The quantum calculations logically give a description of the covalent bonds at the origin of the stability of UO_2^{2+} (Section 4.4). This and other usual qualitative pictures of chemical reactivity are compared for the neighbour actinides of U. The hydration of UO_2^{2+} was recently modelled by taking into account the influence of water beyond the first hydration layer (Section 4.5). Static modelling of two-sphere clusters (Section 4.5.2, Figure 10) has been compared to experiments (Figure 11). This two sphere method has also been tested on fluoride (Section 4.5.3) and acetate (Section 4.5.4, Figure 12) complexes of UO_2^{2+}. In principle, a better way to model bulk liquid water is molecular dynamics (Section 4.6). Car-Parrinello quantum molecular dynamics (CPMD) simulations have been published for the hydration of UO_2^{2+} and its first hydrolysis (Section 4.6.1). Classical molecular dynamics (CℓMD) have also been used to simulate the hydration of UO_2^{2+}, but more details are published for La^{3+} (Section 4.6.2): the geometries of these two central cations are quite different. The hydration of ions with tetrahedral geometries is still an open question (Section 4.7). Finally in the conclusion (Section 5) we point out useful pieces of information that can be extracted from the above molecular modelling methods.

3. AQUEOUS CHEMISTRY OF URANIUM

Hydrolysis, complexation and redox equilibria determine which aqueous chemical species of uranium are formed in equilibrium conditions and in which proportions ("speciation"). In this section we describe these reactions outlining general chemical trends and ideas that are commonly used to explain the aqueous chemistry of uranium. The equilibrium proportions of the aqueous species are calculated from equilibrium constants and standard potentials of redox couples, or equivalently, Gibbs' energy changes. Ways to obtain -select, measure- these thermochemical data are outlined here, together with thermochemical data bases and concepts currently used by solution chemists. These concepts will also be used elsewhere in this chapter, namely for solid solutions and energies of reaction obtained from quantum calculations.

3.1 THE AQUO IONS

3.1.1 Uranium in the Actinide Series, Hard Ions in the Periodic Table

Uranium is the actinide in column 6 of the periodic table. It can be oxidised up to the +6 oxidation state -U(VI)- which is its thermodynamically most stable oxidation state in many media including aqueous solutions. Similarly, the other light elements from the

beginning of line seven display the group oxidation state up to and including neptunium, the actinide in column seven (Figure 1), while in line six, the 4-f block elements follow this trend only as far as cerium, the lanthanide in column four.

The U, Np, Pu, and Am light actinides can be thermodynamically stable in oxidation states 3 to 6 as An^{3+}, An^{4+}, AnO_2^+ and AnO_2^{2+} aquo ions respectively in non-complexing aqueous solutions.[1] Their most stable oxidation states are their group oxidation state up to uranium (Np(VII) can be prepared, but it oxidises water). The group oxidation state is observed across the series for increasing redox potential conditions. Simultaneously the thermodynamics stability of the +3 oxidation state increases from Pa to the heavier actinides. As a result Pu^{3+} is quite stable in non-oxidising acidic conditions, Am and the heavier actinides are thermodynamically stable essentially in the +3 oxidation state in aqueous solutions, with the exception of No^{2+}; nevertheless, Am(IV to VI) and Cm(IV) have been prepared in very oxidising complexing conditions. The light actinides are more easily oxidised than the lanthanides.[2] Stronger attraction by the nuclei and more efficient shielding from the influence of the ligands for the valence electrons of the lanthanides as compared at least to the light actinides are believed to be responsible for this difference. This would also account for the slightly harder[3] character of the lanthanides as compared to the actinides. However, the stabilities of the linear AnO_2^{z-4} actinyl molecular cations (z = 5 or 6) are essentially originated in the $An{\equiv}O_{yl}$ covalent bonds: for these actinyl species, hardness should be understood only for the equatorial ligands, including the HO^- and O^{2-} ions of hydrolysed water.[4] Equivalently, one can consider that the bare An^{z+} cations are soft for z = 5 and 6 but these An^{z+} cations are not stable: when in contact with water hydrolysis usually produces the hard oxo AnO_2^{z-4} molecular cations.[1] Similarly, it is more difficult to oxidise the f-block elements than the softer d transition elements. The cations of the f-block elements are chemical analogues, when in the same oxidation state, where they have the same charge and similar ionic radii.[1] Furthermore, Y^{3+} and Th^{4+} cations, whose electronic structures display no (or negligible) f-character, are chemical analogues of the lanthanides and actinides ions with the same charges. This suggests electrostatic interactions that do not depend significantly on the detail of the electronic configuration. However, this simple picture has exceptions, and it might even not be a completely correct explanation. As counter-examples one can cite that UF_6 is covalent -even though F^- is a hard anion-,[3] and that we have calculated[5] none-negligible charge transfer on the $U\text{-}OH_{hydroxyl}$ bonds in

[1] Pa(V) is an exception among the actinides(V): PaO_2^+ is not the Pa(V) aquo ion. [Siboulet 2008, Toraishi 2006, Vitorge 2007]. Consequently Pa(V) is not a chemical analogue of the transprotactinians(V).

[2] The light actinides can be in higher oxidation states than the lanthanides in the same column at constant redox potential of the solution.

[3] Hard ions behave as (hard) spheres of constant charges. They usually form bonds with ionic character: hard cations usually form strong ionic bonds with hard anions.

[4] The first hydrolysis of H_2O gives HO^-, the second gives O^{2-}.

[5] In this chapter, most quantum calculations were done with Density Functional Theory (DFT) in the form of the gradient-corrected hybrid B3LYP [Becke 1993] as implemented in the Gaussian 03 suite of programs [Gaussian 03] with the Effective Core Pseudo-potentials and basis sets described in Ref. [Ismail 1999, Siboulet 2006 and 2008]. Charges were calculated using the Natural Population Analysis Software NBO [Reed 1988, Glendening 1998] as implemented in Gaussian 03 for comparing the charges; but for charges of actinides we used the NBO5.0 version modified to include 6d

$UO_2(OH)_i(H_2O)_j^{(2-i)+}$ molecules.[6] Conversely Pa is a true f-element,[7] but Pa(V) is not a chemical analogue of the other (AnO_2^+) An(V) ions. PaO_2^+ is clearly not the dominating Pa(V) aqueous cation. It is certainly protonated as $PaOOH^{2+}$ at pH = 0, in equilibrium with non-negligible proportions of Pa(V) mono-cations, possibly tetrahedral $Pa(OH)_4^+$, rather than $PaOOH(OH)^+$ or $PaO(OH)_2^+$ [Siboulet 2008, Toraishi 2006].

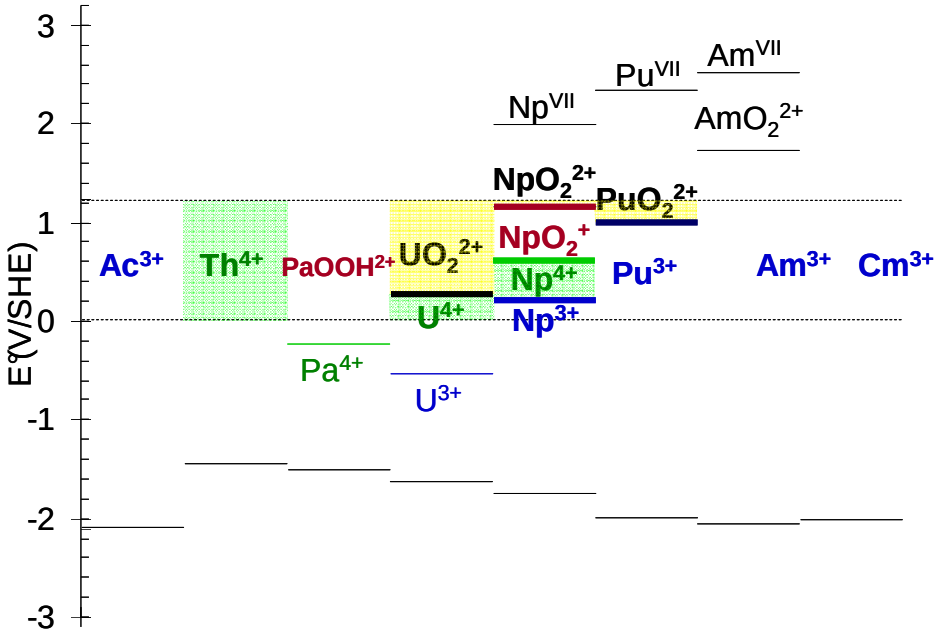

Figure 1. Predominant oxidation states of actinides

at pH 0. The horizontal lines are the (E°) standard potentials of the redox couple for the two species written below and above the line in aqueous solution (I = 0 and 25°C).[9] The subscript (aq) is omitted for simplicity in this chapter when there is no ambiguity. The species written on the figure predominate in the (E) redox conditions between the two (E°) horizontal lines plotted above and below the name of the species. The upper and lower parts of the diagrams do not correspond to equilibrium conditions: water is oxidised (into O_2(g)) or reduced (into H_2(g)) above and below the (1.229 V/SHE) upper and (0 V/SHE) lower dashed lines respectively. The Pu^{4+} predominance domain is within the thickness of the Pu^{3+}/PuO_2^{2+} horizontal line. Non-predominating species do not appear on the figure; but can predominate in other chemical conditions: UO_2^+ typically predominates at about pH = 4 (Figure 2).

Such protonation reactions are not known for AnO_2^{z-4} actinyl ions of the other actinides, probably because this would require too high an acidity in water, where the

in the valence space.

[6] The attractions between anions and cations of high charge/(ionic radius) radii might be sufficient to give small enough bond distances for allowing orbital overlap, besides the other conditions required to form covalent bonds. This is certainly a limit of the qualitative hardness concept.

[7] The bonds formed by Pa(V) usually have a dominant f-character, while for Th(IV) and the lighter actinides they have negligible or minor f-character; in this respect Pa is the first "true" f-element.[1]

concentration of H^+ is necessarily limited. Note that the lower stability of PaO_2^+ destabilizes Pa(V); conversely the high stabilities of the other AnO_2^{z-4} actinyl ions stabilize the oxidation states five and six (Figure 1).[1]

3.1.2 The Redox Potentials of the Uranium Couples

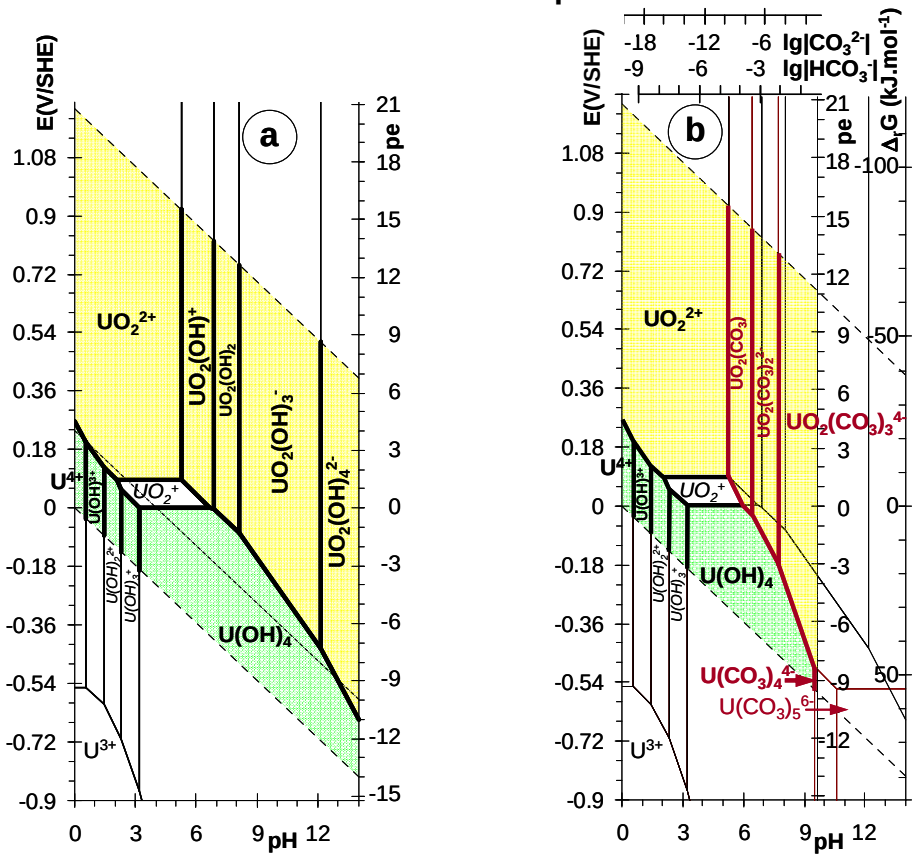

Figure 2. Pourbaix predominance diagrams

of uranium aqueous species in non-complexing media (a) and for P_{CO_2} = 0.01 atm (b). T = 25℃, I = 0, $[U]_t \leq 10^{-9.5}$ mol.ℓ$^{-1}$. E also corresponds to pe and $E_{1/2}$, which in turn correspond to E° and $\Delta_r G°$.[8,18] The (a) hydrolysis diagram is reproduced (thin black lines) in the (b) carbonate diagram to show the effect of complexation. The upper and lower parts of the diagrams do not correspond to equilibrium conditions: water is oxidised (into O_2(g)) or reduced (into H_2(g)) above and below the upper and lower dashed lines respectively.[14] Similarly, adding carbonate by increasing the pH at fixed CO_2 partial pressure (P_{CO_2})[27] results in bicarbonate activities $\left(\left|HCO_3^-\right|\right)$ higher than the solubility of $NaHCO_3$ for pH > 9.7 (right part of diagram b)[28]. The reduction of CO_2 and its HCO_3^- and CO_3^{2-} less acidic forms is ignored. The stabilities of the $U(OH)_2^{2+}$, $U(OH)_3^+$ and UO_2^+ italicized species are not well known (see text).[12,24] Concentrations along the mixed dashed line are given in Figure 3.

The relative thermodynamic stability of two oxidation states is accounted for by E°,

the standard potential of the redox couple, or equivalently $\Delta_r G°$, [8] the Gibbs' energy of the reduction reaction in the reference state.[9] The -usually measured- values of the thermodynamics parameters[10] depend on the relative stabilities of the species, here the binding energy for the last valence electrons of the reduced species (ionization energies) and the balance of the hydration energies of the reduced and oxidised species.

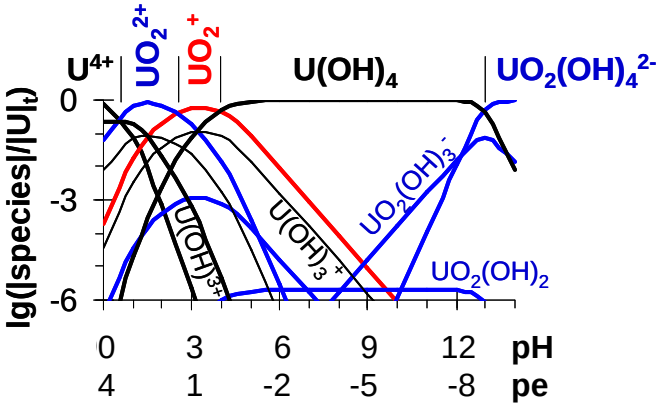

Figure 3. Sillén activity diagram

for uranium in non complexing aqueous solutions**.** T = 25℃, I = 0, $[U]_t < 10^{-9.5}$ mol.ℓ$^{-1}$ for pe = 4 - pH, conditions corresponding to the mixed dashed line in Figure 2a. |species| is the activity of the species written on the diagram and it is equal to its concentration, since the curves are calculated at zero ionic strength: $|U|_t$ is the total concentration of uranium. The predominating species are bolded and written on the top of the figure. The concentrations of $U(OH)_3^+$ and $U(OH)_2^{2+}$ (thin lines, the name of the later is not written on the figure for clarity) might very well be overestimated here, since their thermodynamic stabilities have been roughly estimated (see text).[12]

Since this last term is very important, the standard redox potentials of aqueous species are not necessarily correlated with the ionization energies.[11] Furthermore, the

[8] $\Delta rG° = -n\,F\,E°$, where n is the number of the e^- exchanged electrons, and F the Faraday number. Subscript r is for "reaction". Superscript ° is for "in the reference state". Typically, $\Delta_r G^0_{UO_2^{2+}/U^{4+}} = -2FE^0_{UO_2^{2+}/U^{4+}}$ for the UO_2^{2+} + 2 e^- + 4 H^+ ⇆ U^{4+} + 2 H_2O redox equilibrium –i.e. exchange of electron e^-. E, the potential of the solution can be measured *v.* a reference electrode.[18] Its equilibrium value is (Nernst Equation) $E = E^0_{UO_2^{2+}/U^{4+}} + (E_N/2)\,\lg\left(\left|UO_2^{2+}\right|\left|H^+\right|^4/\left|U^{4+}\right|\right)$, where $E_N = (R\,T\,\ln(10))/F$ = 59.16 mV at 25℃, R is the gas constant, T the tem perature (Kelvin) and |i| the activity of Species i. Nernst Equation is classically re-written as $K^0_{UO_2^{2+}/U^{4+}} = \left|U^{4+}\right|/\left(\left|UO_2^{2+}\right|\left|H^+\right|^4\left|e^-\right|\right)$ by defining $K^0_{UO_2^{2+}/U^{4+}}$ as $\Delta_r G^0_{UO_2^{2+}/U^{4+}} = -2FE^0_{UO_2^{2+}/U^{4+}} = -RT\ln\left(K^0_{UO_2^{2+}/U^{4+}}\right)$ and $\lg|e^-| = E/E_N$ corresponding to the more general definitions $\Delta_r G° = -R\,T\ln(K°) = -n\,F\,E°$, and $E = E_N \lg|e^-| = -E_N$ pe. The pe scale is written on Figure 2 together with the E scale.

[9] The activities are 1 for all the species in the reference state of aqueous solutions. This is Pure Liquid Water: $|H_2O| = 1$. Typically, $E^0_{UO_2^{2+}/U^{4+}}$ is E for pH = 0 ($|H^+| = 1$) and $\left|UO_2^{2+}\right| = |U^{4+}|$.

[10] $\Delta_r G°$ and E° are thermodynamic constants. [8]

[11] Similarly, it has been proposed to define hardness quantitatively from the chemical potential of the electron; but it is no easily linked to μ_{e^-}, the thermodynamic potential of the electron –hence to E, the redox potential- as defined in Footnote.[18]

relative thermodynamic stabilities of the oxidation states can be modified by hydrolysis or complexation, which stabilizes the oxidation state of the most thermodynamically stable complexes. $\Delta_r G°$ is for a given medium, here pure liquid water at pH = 0,[9] where the solutes are hydrated and possibly hydrolysed.

Uranium can be in oxidation states +3 to +6. However, only U^{4+} or UO_2^{2+} are predominating in aqueous solutions: U^{3+} reduces water, and UO_2^+ disproportionates in most (E, pH) equilibrium conditions as shown by the Pourbaix' diagram (Figure 2)[12]. Such diagrams show only the predominating species; other species are present in equilibrium with these (Figure 3).

As expected, U(IV) predominates in reducing conditions, while in less reducing and oxidising conditions it is oxidised into U(V) or U(VI). The relative stabilities of uranium aquo ions vary with pH, since the UO_2^{2+} uranyl ion can hydrolyse.[13] The (electroactivity) domain of liquid water is also limited by its oxidation and reduction.[14] Nevertheless, U^{3+} can be detected -typically by cyclic voltametry- because the reduction of water is sufficiently slow.

Similarly the equilibrium potential of the UO_2^{2+}/UO_2^+ redox couple can be measured in non-equilibrium conditions, typically at pH = 0 to avoid the hydrolysis of UO_2^{2+} [Capdevila 90]. This slow kinetics is due to the high strength of the $U{\equiv}O_{yl}$ bond. For this reason, no isotopic exchange is observed for O_{yl} with an O atom of bulk water within the time scale of laboratory experiments. When needed -as typically for NMR measurements- such exchange is classically promoted by exposure to UV light.

The redox potential does not depend on pH (horizontal lines between UO_2^{2+} and UO_2^+, and between UO_2^+ and $U(OH)_4(aq)$ in Figure 2) for the redox couples of species being in the same degree of hydrolysis.[13] Conversely, the redox properties of uranium depend strongly on pH for most of the uranium species.

3.2 Hydrolysis (Pourbaix' Diagram)

Uranium is stabilised in the oxidation state six compared to U(IV) on increasing pH from pH = 0, because UO_2^{2+} is more extensively hydrolysed than U^{4+} at the same pH (Figure 2 a).[15] However, U^{4+} is more easily hydrolysed than UO_2^{2+}: U^{4+} and UO_2^{2+} are first

[12] The size of the UO_2^+ aqueous predominance domain is not well established, because the thermodynamic stability of $U(OH)_4(aq)$ is not accurately known (see Section 3.2): if $U(OH)_4(aq)$ is more stable than estimated below, its predominance domain is bigger, hiding the neighbouring ones and suppressing that of UO_2^+.

[13] The degree of hydrolysis is the number of HO^- ligands plus twice the number of O^{2-} ligands,[4] a definition convenient for solution chemistry, which does not distinguish between oxo-hydroxo-species with the same degree of hydrolysis, because the $[UO_j(OH)_{6-2j-z}^{z+}]/[UO_i(OH)_{6-2i-z}^{z+}]$ concentration ratios between two such species is constant: it is the constant of the $UO_j(OH)_{6-2j-z}^{z+} \leftrightarrows UO_i(OH)_{6-2i-z}^{z+} + (i-j)H_2O$ equilibrium, where the activity of water is constant in a given aqueous solution at constant temperature and pressure.

[14] The redox reactions are $H^+ + e^- \leftrightarrows 0.5\ H_2(g)$ and $0.5\ O_2(g) + 2\ e^- + 2\ H^+ \leftrightarrows H_2O$ for the limits of the water electroactivity domain.

[15] UO_2^{2+} is U^{6+} hydrolysed four times, which increases the thermodynamic stability of U(VI) as compared to less hydrolysed U

hydrolysed into $U(OH)^{3+}$ and $UO_2(OH)^+$ at pH (0.54 ± 0.06) and (5.2 ± 0.3) respectively. These (0.54 and 5.2) $pH_{1/2}$ numerical values appear as vertical lines in the Pourbaix' diagram (Figure 2).[16] They also give the corresponding hydrolysis equilibrium constants and, equivalently, ($\Delta_r G$) Gibbs energies of reactions:[17] the horizontal scale has the meanings of both activity (pH) and energy ($\Delta_r G$) through $pH_{1/2}$. Similarly the vertical scale represents both activity (pe or equivalently E)[18] and energy ($\Delta_r G$ or equivalently E°), [19] where e^-, the electron, is exchanged instead of H^+.[20] The stabilisation of U(VI) with pH does not dramatically increase the predominance domain of U(VI) over U(IV), because the U(VI)/U(IV) border lines have similar (E(pH)) slopes than the limiting lines of the water electroactivity domain. These slopes correspond to the (1 ± 1) e^- per H^+ stoichiometry of the redox reactions.[20,21]

On increasing pH, UO_2^{2+} is further hydrolysed into $UO_2(OH)_i^{(2-i)+}$ for i ≤ 4. This limiting i (≤ 4) value is caused by the repulsion between the HO^- ligands. This also predicts quite regular HO^- additions with increasing pH; but this is still an open question in liquid water.

---

species.[13]

[16] $pH_{1/2}$ is the pH at the half-reaction points, i.e. the pH for which there is the same amount of product and reactant. For a typical equilibrium $UO_2(OH)_{i-1}^{(3-i)+} + H_2O \leftrightarrows UO_2(OH)_i^{(2-i)+} + H^+$, where ${}^*K_i^0 = \left|UO_2(OH)_i^{(2-i)+}\right| \, |H^+| \, / \, \left|UO_2(OH)_{i-1}^{(3-i)+}\right|$, $pH_{1/2,i}$ is the pH, where $\left|UO_2(OH)_i^{(2-i)+}\right| = \left|UO_2(OH)_{i-1}^{(3-i)+}\right|$. Superscript * is a classical notation to stress that the reaction is written with the (H_2O) protonated form of the (HO^-) ligand, here leading to simple exchange of (H^+) proton. It appears that $-\lg {}^*K_i^0 = pH_{1/2,i}$. When the ionic strength is constant, |i| is set equal to [i], the concentration of species i.

[17] Typically ${}^*\Delta_r G_i^0 = -R\,T\ln {}^*K_i^0$ for the equilibrium in Footnote [16]. R T ln(10) = 5.71 kJ.mol^{-1} at T = 298.15 K

[18] Various equivalent notations are used: E and pe, and E° and $\Delta_r G$.[8,20] They can be made consistent with thermodynamics conventions as follows. E can be measured *v.* a reference, the Standard Hydrogen Electrode (SHE) (E is often noted E_h, where subscript h is for *v.* SHE), similarly the origins of pe and $|e^-|$ are set by the SHE convention. For this reason $|e^-|$ is not –it is actually far from- the concentration of the solvated electron [e^-(aq)]. The SHE corresponds to the $H^+ + e^- \leftrightarrows 0.5\ H_2(g)$ equilibrium: $\Delta_r G_{SHE}^0 = 0$, where $\Delta_r G_{SHE}^0 = 0.5\Delta_f G_{H_2(g)}^0 - \Delta_f G_{H^+(aq)}^0 - \Delta_f G_{e^-}^0$. Subscript f is for "formation": $\Delta_f G_i^0$ is another notation for μ_i^0, the standard chemical potential of species i, |i| is defined as $\mu_i = \mu_i^0 + R\,T\ln|i|$, where μ_i is the chemical potential of species i. $\Delta_f G_{H_2(g)}^0 = 0$ because $H_2(g)$ is the reference state for Element H. Consequently $\Delta_f G_{e^-}^0 = -\Delta_f G_{H^+(aq)}^0$. Similarly $\Delta_f H_{e^-}^0 = -\Delta_f H_{H^+(aq)}^0$. $\Delta_f G_i^0$ and $\Delta_f H_i^0$ are usually tabulated in thermochemical data bases at 25°C; while S_i^0 (not $\Delta_f S_i^0$) is tabulated at 25°C: $S_{H_2(g)}^0 = 130.680 \pm 0.003$ J.K^{-1}.mol^{-1}, not 0. $\Delta_f G_i^0$ and $\Delta_f H_i^0$ are zero only if i is the reference state of the corresponding element. However, $\Delta_f G_{H^+(aq)}^0 = 0$ kJ.mol^{-1} and $\Delta_f H_{H^+(aq)}^0 = 0$ kJ.mol^{-1} are also tabulated in some thermochemical databases; in that case $\Delta_f H_{e^-}^0 = 0$ kJ.mol^{-1} and $\mu_{e^-}^0 = \Delta_f G_{e^-}^0 = 0$ kJ.mol^{-1}, from which $\mu_{e^-} = F\,E$.[8]

[19] E is the redox potential of the solution, E° the normal potential of a redox couple and E°the standard potential of the redox couple, i.e. E° in the standard conditions, namely $\Delta_r G° = -n\,F\,E°$, [8] and $\Delta_r G = -n\,F\,E°$.

[20] The example in footnote[16] can be extended to the exchange of any species. For redox equilibria -exchange of an electron e^- instead of H^+- e^- (pe)[8] has the role of H^+ (pH): lg K° = $pe_{1/2}$ (or equivalently E° = $E_{1/2}$).[8] In the $UO_2^{2+} + 2\,e^- + 4\,H^+ \leftrightarrows U^{4+} + 2\,H_2O$ redox equilibrium both H^+ and e^- are exchanged. By definition of the activities $\Delta_r G°$, E° and K° are the values of $\Delta_r G$, E and K when all the activities are 1. Consequently $E_{UO_2^{2+}/U^{4+}}^0$ is also $E_{1/2}$ at pH = 0: the value of E for $|U^{4+}| = \left|UO_2^{2+}\right|$, and $|H^+| = 1$. $E_{1/2}$ (linearly) depends on the pH; the slope is -i E_N/n, where i/n is the number of H^+ exchanged per e^-, the ratio of the stoichiometric coefficients in the redox equilibrium.

[21] The redox reactions are those given in Footnote [14] and $UO_2(OH)_i^{(2-i)+} + 2\,e^- + (4+i-j)H^+ \leftrightarrows U(OH)_j^{(4-j)+} + (2+i-j)H_2O$ with i-j = -1 ± 1 in most pH conditions (Figure 2).

Conversely, it is not known why $U(OH)_4(aq)$ has a larger pH predominance domain than other $U(OH)_i^{(4-i)+}$ species. The value of ${}^*K_{1,IV}$, the first hydrolysis constant for the formation of $U(OH)^{3+}$ is well accepted, but the thermodynamic stabilities of the $U(OH)_i^{(4-i)+}$ species are not well established for i = 2 and 3. The value of $lg\,{}^*K_{1,IV}$ is taken here from the original NEA TDB review [Grenthe 1992], where no values were selected for any other $U(OH)_i^{(4-i)+}$ species (i > 1). Grenthe *et al.* only pointed out that the (${}^*\beta_{4,IV}$) hydrolysis constant for the formation of $U(OH)_4(aq)$ should reflect the ($10^{-9.5}$ mol.ℓ^{-1}) experimental solubility of uranium in the chemical conditions, where $U(OH)_4(aq)$ is the major U species. Based on this idea and using K_{s0,PuO_2}, the solubility product of the analogous Pu(IV) compound (K_{s0,UO_2} is poorly known, and the experimental solubilities of all the actinides(IV) are similar) give $lg\,{}^*\beta_{4,IV} = -7.5$ [Vitorge 2003], a value higher than the (-10 ± 1.4) value selected by the last update of the NEA review.[22] An uncertainty of about ± 2.9 on our $lg\,{}^*\beta_{4,IV} = -7.5$ value encompasses the (-10 ± 1.4) NEA value. These large uncertainties are partially due to the solubility of U (for ±1)[22] and mostly to K_{s0,UO_2}. It propagates into the size of the predominance domains of $U(OH)_4(aq)$ and of its neighbouring species, including UO_2^+ which already has a small predominance domain (Figure 2). Whatever the $lg\,{}^*\beta_{4,IV}$ value within its large uncertainty range, the pH predominance domain of $U(OH)_4(aq)$ is much larger than that of the other $U(OH)_i^{(4-i)+}$ species.[23] As expected this is also true for the other actinides(IV). This high relative stability could very well be caused by favourable hydration geometry, among other possible explanations. This is still an open question. Would similar geometrical or hydration properties also influence the stabilities of other $M(OH)_4^{(z-4)+}$ species?

From ${}^*K_{1,IV}$ and ${}^*\beta_{4,IV}$ we estimated ${}^*K_{2,IV}$ and ${}^*K_{3,IV}$ for the stabilities of the $U(OH)_2^{2+}$ and $U(OH)_3^+$ intermediary species arbitrary assuming regular additions of the HO^- ligands.[24] Now this is only a -usual- hypothesis with no strong scientific basis: $U(OH)_2^{2+}$ and $U(OH)_3^+$ might very well have no predominance domain, especially since they have not really been detected experimentally.[25] In that case $U(OH)_4(aq)$ would have an even larger predominance domain.

---

[22] Using the NEA update value, $10^{-8.5}$ mol.ℓ^{-1} is calculated for the solubility of uranium in neutral and reducing conditions. It is consistent with the ($10^{-9.5}$ mol.ℓ^{-1}) experimental value only thanks to the large uncertainty. K_{s0,AnO_2} is the solubility product of the AnO_2 phase that actually controls the aqueous solubility of An at room temperature. For kinetic reasons this solid is not the most stable solid $AnO_2(cr)$: the solid that actually controls the solubility is currently written $AnO_2(am.,hyd.)$ or $An(OH)_4(s)$, but it might very well be micro-crystalline AnO_2.

[23] The pH length of the predominance domain of $U(OH)_4(aq)$ is $\Delta pH = pH_{1/2,5,IV} - pH_{1/2,4,IV}$, where $pH_{1/2,i,IV} = -lg\,{}^*K_{i,IV}$.[16] $\Delta pH = -lg\,{}^*K_{5/4,IV}$, where ${}^*K_{5/4,IV} = {}^*K_{5,IV} / {}^*K_{4,IV}$ appears to be the constant of equilibrium $2\,U(OH)_4(aq) \leftrightarrows U(OH)_3^+ + U(OH)_5^-$, which indeed reflects the relative stability of $U(OH)_4(aq)$. The exact value of ${}^*K_{1/2,5,IV}$ is not known, for this reason $U(OH)_5^-$ is not taken into account in this chapter: $-lg\,{}^*K_{1/2,5,IV} = pH_{1/2,5,IV} > 12.5$, while here we implicitly used > 14.

[24] We assumed $lg\,{}^*K_{i,IV} = lg\,{}^*K_{i-1,IV} + 0.89$ to estimate $lg\,{}^*K_{i,IV}$ for i = 2 and 3,[25] where 0.89 is chosen to fit $lg\,{}^*K_{1,IV} = -0.54$ and $lg\,{}^*\beta_{4,IV} = -7.5$ (${}^*\beta_{4,IV} = {}^*K_{1,IV}\,{}^*K_{2,IV}\,{}^*K_{3,IV}\,{}^*K_{4,IV}$).

[25] There is no clear experimental evidence of $U(OH)_2^{2+}$ neither $U(OH)_3^+$. Their influence is typically within the uncertainty of experimental solubilities of U(IV).

The particularly easy hydrolysis of U^{4+} is usually explained as follows: electrostatic interactions of anionic ligands –typically, such as HO^-- increase with the charge of the cation, and decrease with the ionic radii. Indeed U^{4+} is more highly charged and smaller than UO_2^+. Consistent with the supposed hard characters of UO_2^+ and HO^-, this electrostatic explanation suggests U-OH purely ionic interactions, which is not supported by quantum calculations (as outlined above):[5] small HO^- (as also F^-) bond to U(VI) with non-negligible covalent character.[6] Nevertheless, U(VI) is a good chemical analogue of the actinides that can be stable (Np(VI), Pu(VI)) -or at least observed (Am(VI))- in the oxidation state six. Since U(VI) is the most stable An(VI) -the easiest one to prepare and study in this oxidation state- it is often used as a representative for the actinides(VI). Conversely, the chemistry of U(III), U(V) and even U(IV) is often predicted by analogies with Am(III), Np(V) and Th(IV) respectively. The actinide[1] aquo cations are more easily hydrolysed in the order:

$$AnO_2^+ << An^{3+} < An^{4+} << AnO_2^{2+}$$

as reflected in their lg^*K_1 values.

$$-11.3 << -6.8 < -5.25 << -0.54$$

3.3. COMPLEXATION

3.3.1. Empirical Correlations of Complexation Constants

The stabilities of the complexes for the actinide cations with hard anionic ligands usually increase in the same order as the stabilities of their soluble hydroxides. Such an assumption should be checked for all the available complexing constants of anionic ligands with the uranium or analogous cations. Unfortunately the scattering of the published numerical values can be substantial for complexing constants, sometimes more important than the difference between different analogous cations. For this reason the data should first be critically evaluated. This has essentially been done by Grenthe *et al.* in the initial critical review of uranium for the NEA-TDB [Grenthe 1992]. Using these selected values, a similar trend is usually found for hydrolysis and complexation

$$An(V) << An(III) \approx An(VI) << An(IV)$$

typically for RO_2^{2-} di-anionic potentially bidentate ligands as deduced from the correlation of K_1^0, the standard formation constant of the $\left(MRO_2^{(z-2)+}\right)$ 1-1 complex as a function of pKa°, the standard acidity product of the $\left(RO_2^{2-}\right)$ ligand (Figure 4) [Vitorge 2007]. Furthermore, the reactivities of the ligands vary in the order

$$S_2O_3^{2-} \approx SO_4^{2-} < HPO_4^{2-} \approx SO_3^{2-} < CO_3^{2-}$$

an usual for hard cations. There is not a single outlier. Nevertheless, such a correlation is empirical. It is certainly originated in several physical phenomena that themselves are correlated to parameters -typically charge/(ionic radius) ratios of the ions- that are not

necessarily clearly identified. The (K_1 *v.* Ka) correlation essentially reflects the order of the bond strength between the metal and the (O) donor atoms of the ligands in the $\left(MRO_2^{(z-2)+}\right)$ 1-1 complexes. $S_2O_3^{2-}$ and CO_3^{2-} form the weaker and stronger complexes, respectively, with the actinide cations. SO_4^{2-} and $S_2O_3^{2-}$ are very similar. CO_3^{2-} and SO_4^{2-} complexes have been extensively studied, typically for their chemical importance in environmental waters, where other inorganic hard anionic ligands -such as F^- and HO^-- can also form complexes with uranium. The K_1(*vs* Ka) log-log correlation also often qualitatively reflects the relative stabilities of higher-order complexes.

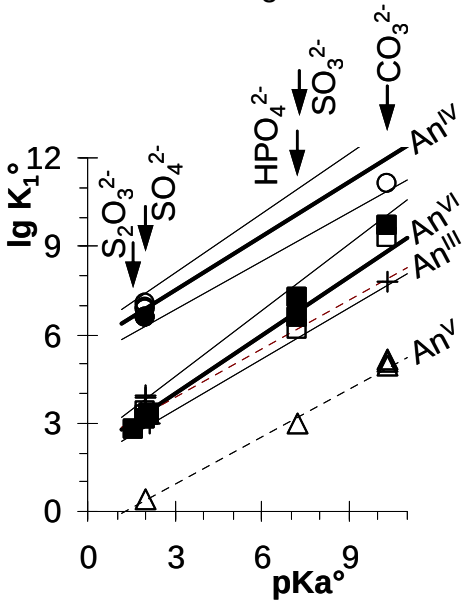

Figure 4. Complexing constants,

K_1, of U (black points) and other actinides in Oxidation States 6 (squares), 5 (triangles), 4 (circles) and 3 (crosses) with bidentate di-anionic ligands (L = RO_2^{2-} = $S_2O_3^{2-}$, SO_4^{2-}, HPO_4^{2-}, SO_3^{2-} and CO_3^{2-} as a function of Ka, the acidity constant of L. $K_1° = \left|MRO_2^{(z-2)+}\right| / (|M^{z+}|\left|RO_2^{2-}\right|$, pKa = -lg Ka° and Ka° = $|H^+|\left|RO_2^{2-}\right| / \left|HRO_2^-\right|$.

3.3.2 Carbonate Complexes of U(VI)

A maximum of three carbonate ligands can be placed in the first coordination sphere -actually the equatorial plane- of UO_2^{2+}: in the $UO_2(CO_3)_3^{4-}$ limiting complex of U(VI) the three CO_3^{2-} ligands are bidentate, while some can be monodentate in solids (Figure 5). In all these structures the first coordination layer of UO_2^{2+} is saturated with O atoms of CO_3^{2-} ligands: there is no other ligand or water molecule in the first layer.

Uranium can be stabilized in the oxidation state +5 as a carbonate complex. In concentrated carbonate aqueous solutions, where the limiting complexes predominate for uranium in all its oxidation states, the disproportionation equilibrium of U(V) is

$$2\ UO_2(CO_3)_3^{5-} + 2\ CO_2(g) \rightleftarrows UO_2(CO_3)_3^{4-} + U(CO_3)_5^{6-}$$

which shows that U(V) is stabilized on decreasing P_{CO_2}, providing the carbonate concentration is high enough to avoid the dissociation of the U(V) limiting complex, $UO_2(CO_3)_3^{5-}$. This is indeed feasible for $P_{CO_2} = 10^{-6}$ atm (not shown on Figure 2 b), and the potential of the U(VI)/U(V) redox couple has been measured [Capdevila 1990], as for the Np, Pu and Am series of actinides.

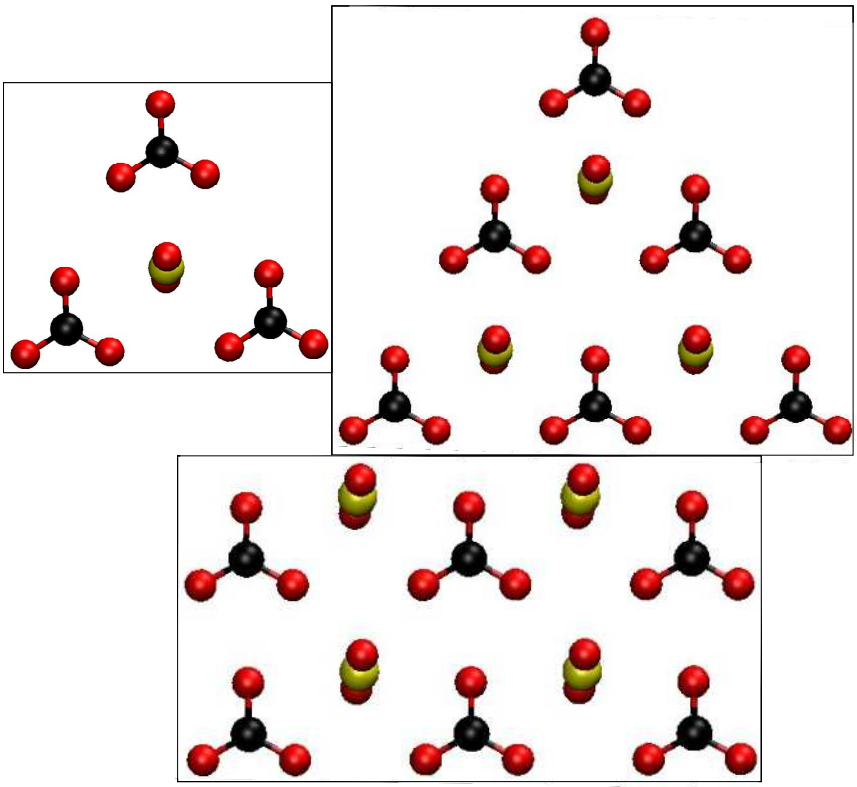

Figure 5. CO_3^{2-} **coordination to** UO_2^{2+} in aqueous complexes $UO_2(CO_3)_3^{4-}$ (left) and $(UO_2)_3(CO_3)_6^{6-}$ (right), and in solid rutherfordine (bottom): schematic views, where the C (black) and O (red) atoms are in the equatorial plan of linear UO_2^{2+}. These schematic geometries were constructed with Molden [Schaftenaar 1991] and drawn with VMD [Humphrey 1996].

This set of data allows the comparison of the stabilities for such a series of actinyl aqueous complexes. The shift of the standard potentials for the An(VI)/An(V) redox couple between non-complexing and concentrated carbonate aqueous solutions provides the $(\beta^0_{3,V}/\beta^0_{3,VI})$ ratio of the stability constants of the limiting complexes.[26] This is

[26] $E = E° + E_N \lg(|UO_2^{2+}|/|UO_2^{+}|) = E° + E_N \lg(\beta^0_{3,V}/\beta^0_{3,VI}) + E_N \lg(|UO_2(CO_3)_3^{4-}|/|UO_2(CO_3)_3^{5-}|)$, where $\beta^0_{3,VI} = |UO_2(CO_3)_3^{4-}| / (|UO_2^{2+}|\ |CO_3^{2-}|^3)$ and $\beta^0_{3,V} = |UO_2(CO_3)_3^{5-}| / (|UO_2^{+}|\ |CO_3^{2-}|^3)$. In non-complexing media E is measured for $[UO_2^{2+}] =$

used to determined complexation constants. The $(\beta^0_{3,V}/\beta^0_{3,VI})$ ratio is the constant of the

$$UO_2(CO_3)_3^{4-} + UO_2^+ \leftrightarrows UO_2(CO_3)_3^{5-} + UO_2^{2+}$$

exchange equilibrium. When replacing U by another An, it decreases slightly with the atomic number, though its variations might very well be within the uncertainty, consistent with the analogy between the actinides (Figure 6). $\beta^0_{3,VI}$ and $\beta^0_{3,V}$ clearly decrease across this actinide series.

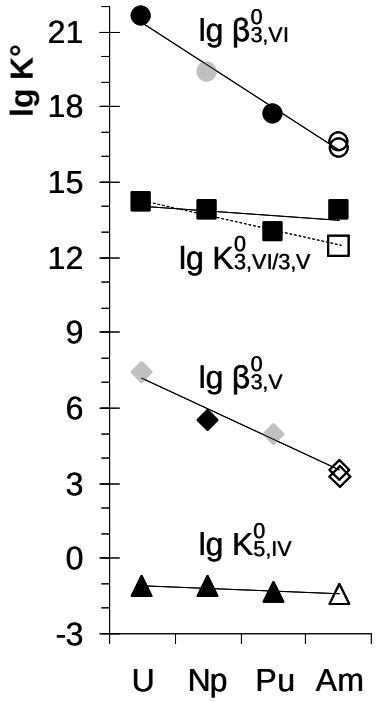

Figure 6. Stabilities of limiting carbonate complexes across the actinide series
as measured by the (K°) standard equilibrium constants [Lemire 2001] for $UO_2^+ + 3\ CO_3^{2-} \leftrightarrows UO_2(CO_3)_3^{5-}$ (K° is $\beta^0_{3,V}$, diamonds), $UO_2^{2+} + 3\ CO_3^{2-} \leftrightarrows UO_2(CO_3)_3^{4-}$ (K° is $\beta^0_{3,VI}$, circles), $UO_2^{2+} + UO_2(CO_3)_3^{5-} \leftrightarrows UO_2^+ + UO_2(CO_3)_3^{4-}$ ($K^0_{3,VI/3,V} = \beta^0_{3,VI} / \beta^0_{3,V}$, squares) and $U(CO_3)_4^{4-} + CO_3^{2-} \leftrightarrows U(CO_3)_5^{6-}$ ($K^0_{5,IV}$, triangles) directly measured (black points), deduced from thermodynamic cycles (grey points) or estimated from linear correlations (white points and lines).[26]

This is attributed to the decrease of the ionic radii, assuming that steric repulsion dominates this trend as a result of the saturation of the first coordination sphere by the donor atoms of the ligands for limiting complexes. Such a decrease is not specially

$[UO_2^+]$, while in carbonate media E is measured for $[UO_2(CO_3)_3^{4-}] = [UO_2(CO_3)_3^{5-}]$. The shift of E between the two media appears to be $E_N \lg(\beta^0_{3,V}/\beta^0_{3,VI})$, which gives the $(\beta^0_{3,V}/\beta^0_{3,VI})$ ratio of the complexing constants of the complexes in each oxidation state.

observed for $K^0_{5,IV}$, the stepwise formation constant of the An(IV) limiting complexes, even though the first coordination spheres are certainly saturated by the donor atoms of the ligands. The carbonate limiting complexes of the Actinides(IV) are only formed in concentrated carbonate aqueous solutions of high ionic strength, which are not really (pure) liquid water. At high ionic strength the very highly negatively charged $An(CO_3)_5^{6-}$ complexes are stabilised by counter-ion.

3.3.3 Sulphate Complexes of U(VI)

The $UO_2(SO_4)_3^{4-}$ limiting complex is formed only in concentrated aqueous solutions of high ionic strength [Vercouter 2008]. The coordination of the not very strong SO_4^{2-} ligand to UO_2^{2+} is not very rigid as reflected in molecular modelling [Hennig 2007, Vallet 2007] and spectroscopic [Neuefeind 2004; Hennig 2007] studies, which proposed both mono and bidentate coordinations: several conformations of the sulphate complexes might be stable in solution, where the water hydrogen-bond networks can very well destabilize the coordination of monodentate tetrahedral SO_4^{2-} in $UO_2(SO_4)_3^{4-}$. This also depends on the water activity, which varies with the ionic strength.

3.3.4 Uranium in Ground-Waters

The carbonate contents of ground-waters –typically at 0.01 atm CO_2 partial pressure (P_{CO_2})-[27] can be sufficient to stabilize U(VI) in the form of carbonate complexes, hence dissociating the soluble U(VI) hydroxides that would form in the same pH conditions but at lower P_{CO_2} (Figure 2 b). Conversely, the carbonate complexes of U(IV) have virtually no influence,[28] *i.e.* they are not stable enough to destabilize the hydroxides of U(IV), while in acidic conditions the ligand is protonated. This is surprising since smallest more highly charged U^{4+} is expected to form stronger complexes. Indeed up to 5 CO_3^{2-} ligands can coordinate to U(IV), while only 3 to U(VI). The predominance domain of U(VI) increases with increasing carbonate concentration, and consequently the domain of U(IV) decreases (Figure 2 b). These apparent higher stabilities of the U(VI) carbonate complexes as compared to U(IV), should instead be due to the high stability of $U(OH)_4$(aq), which limits the formation of the carbonate complexes of U(IV): it is certainly better considering that $U(OH)_4$(aq) is stabilized on decreasing P_{CO_2}.

As expected, the S-containing ligands have a smaller influence, because neither SO_4^{2-} nor $S_2O_3^{2-}$ forms very strong complexes, and because SO_3^{2-} is reduced in equilibrium conditions, where uranium is stable in the oxidation state +4 [Vitorge 2007]. Neither $S_2O_3^{2-}$ nor SO_3^{2-} predominate in aqueous equilibrium conditions, where the

[27] Increasing pH at constant P_{CO_2} increases the concentrations of HCO_3^- and CO_3^{2-}(aq) as a result of Equilibria $CO_2(g) + H_2O \leftrightarrows HCO_3^- + H^+$, and $HCO_3^- \leftrightarrows CO_3^{2-}(aq) + H^+$.

[28] The carbonate complexes of U(IV) are predominating in non-equilibrium conditions (over-saturation of HCO_3^-) in Figure 2 b, but they have been prepared in concentrated carbonate solutions of high ionic strengths. For this reason, they are outside the zero ionic strength Pourbaix diagram (Figure 2 b).

predominating S-containing free ligands are SO_4^{2-} and S^{2-} or their protonated forms. This limits the aqueous activities of the other S-containing ligands and the formations of their complexes.

3.4 THERMODYNAMICS

3.4.1 Thermochemical Data Bases

3.4.1.1. Formation constants

The geochemical behaviour of actinides has been extensively studied for understanding uranium and thorium ore deposits, and more recently for assessing the environmental impact of possible disposals for wastes that contain the U, Pa, Np, Pu, Am or Cm actinides among fission and activation products. The potential radio-toxicities of disposals depend on the solubilities of radio-nuclides, their migrations and their retardations by sorption on minerals, processes that are dependent on the details of the stoichiometries and stabilities of the aqueous species. It is not straightforward to obtain the correct stoichiometries and thermodynamic stabilities of all the relevant aqueous species from the scientific literature, since some inaccurate or even inconsistent data are proposed. This was recognized in the early stage of scientific studies for the management of nuclear wastes: scientists are required to provide a clear picture of the potential radio-toxicity for typically geological deep disposals, avoiding polemics on such calculated predictions. Starting with uranium [Grenthe 1992], the Thermochemical Data Base project of the Nuclear Energy Agency (NEA-TDB) organised the reviewing of the published experimental data.

The equilibrium constants and redox potentials selected by this NEA-TDB review are adequate for a reliable modelling of uranium inorganic chemistry in most equilibrated ground-waters, and the results of the NEA-TDB reviews are now well accepted as a reference critical review essentially for inorganic aqueous chemistry and solubility at room temperature, but the NEA-TDB reviews propose data only when convincing experimental validations have been published. There is therefore a gap between this restricted set of quantitative validated thermochemical data and qualitative chemical knowledge. Using only the validated -but restrictive- set of NEA-TDB thermochemical data can give incorrect calculated solubilities and aqueous concentrations, typically when no data have been selected for a species that can predominate in relevant chemical conditions: it is necessary to estimate the missing values of equilibrium constants and associated uncertainties. These estimates can be based on information given in the text of the NEA-TDB books, or on correlations as exemplified above (Figure 4). Experimental determinations of equilibrium constants are explicitly used -together with auxiliary thermochemical data- to build the NEA-TDB, and these experimental and auxiliary data are provided: this is not always documented in other data bases. These data and the qualitative explanations of their selections are needed to keep the consistency of the data base, when adding -or modifying- data, as we typically did above (Section 3.2) for the stability of $U(OH)_4(aq)$: we chose its stability to reproduce experimental solubilities, which are not thermochemical data directly tabulated in the final data base.

3.4.1.2 Estimating Missing Formation Constants.

The NEA Np-Pu review for carbonate complexes [Lemire 2001] proposed that even when the differences between thermo-chemical data for different actinides are within the scatter of the published complexing constants, it can still be possible to obtain a better picture by comparing the data from the same laboratory, because many systematic errors cancel out when comparing measurements and interpretations performed with the same methodologies. This is the case for the data illustrated in Figure 6 that show virtually the same trends as the earlier work of Capdevila *et al.* [Capdevila 1990]. Such a comparison supports the idea of using analogies; in this case, linear regressions with the atomic number account reasonably well for the variations of the (log of the) complexing constants across the actinide series. It is usually proposed that a consideration of the (charge/ionic radius) ratio is sufficient to understand such trends qualitatively, and this implicitly relies on considering the actinides as hard cations. For this reason Th is considered as an analogue of U(IV), despite their quite different electronic configurations. This, and similar comparisons allow us to estimate missing values of complexing constants, or to check whether the orders of magnitudes are reasonable; if not this can indicate an error... or any specific chemical stabilisation of a given complex.

3.4.1.3 Activity Coefficients.

Inconsistencies or scattering of published complexing constants can arise due to systematic errors -or differences in experimental methodologies, calibrations or interpretations- between different laboratories as discussed -and tentatively corrected- by the NEA-TDB reviews. pH calibration is typically at the origin of such problems, because it is not always clear how junction potentials and activity coefficients are treated. The way of calculating the activity coefficients actually gives the practical definition of the reference state -infinite dilution *i.e.* pure liquid water or equivalently "zero ionic strength"-[29] together with concentration units [Stoke 1991]. There is no international convention or agreement on the way to calculate activity coefficients, which makes it difficult to compare published data or perform accurate concentration calculations. However, an empirical formula -the SIT formula- has been proposed and used by the NEA-TDB on Uranium for calculating the activity coefficients.[30] It needs one

---

[29] "Ionic strength corrections" are used to change the numerical values of the equilibrium constants -and other thermodynamic parameters- from the reference state –the solvent (typically pure water)- to the real solution. These corrections indeed essentially depend on the ionic strength, but they are specific to each solution, especially at high ionic strength, as taken into account by the SIT formula.[30]

[30] $\lg \gamma_i = -z_i^2 D + \sum_j \varepsilon_{i,j}\, m_j$ for activity coefficient γ_i of ion i, with charge z_i. $D = \frac{a\sqrt{I_m}}{1+b\sqrt{I_m}}$ is a Debye-Hückel term, where I_m is the ionic strength (subscript m is for $mol.kg^{-1}$, *i.e.* mole per kg of water: water, not solution) at 25°C a = 0.509 and b is arbitrarily fixed equal to 1.5. The summation is over all the species, j, of concentration m_j ($mol.kg^{-1}$); however, $\varepsilon_{i,j} = 0$ when $z_i\, z_j \geq 0$, and $\varepsilon_{i,j}\, m_j$ is negligible when j is not a major species (relatively small values of m_j). When I_m is the result of the concentration (m) of a single salt the formula simplifies: $\lg \gamma_i = -z_i^2\, D + \varepsilon_{i,j}\, m$, where j is the ion of the salt with charge opposite to z_i. For an equilibrium constant, K, $\lg K^\circ = \lg K - \Delta_r z^2\, D + \Delta_r \varepsilon_i\, m$, where Δ_r has the same meaning as in $\Delta_r G = -R\, T \ln K$.

($\varepsilon_{i,j}$) ion-pair empirical interaction parameter per (i,j) pair of ionic species. Many parameters are tabulated and their origins documented in the NEA-TDB books. They can also be *a priori* estimated by analogy, since they should provide only small ionic-strength corrections,[29] and the $\varepsilon_{i,j}$ SIT parameters have similar values for similar ions and are correlated to the charges of the ions (Figure 7), which allow reasonable estimates of the unknown values in most cases: the actinide ions of same charges have similar $\varepsilon_{i,j}$ values.

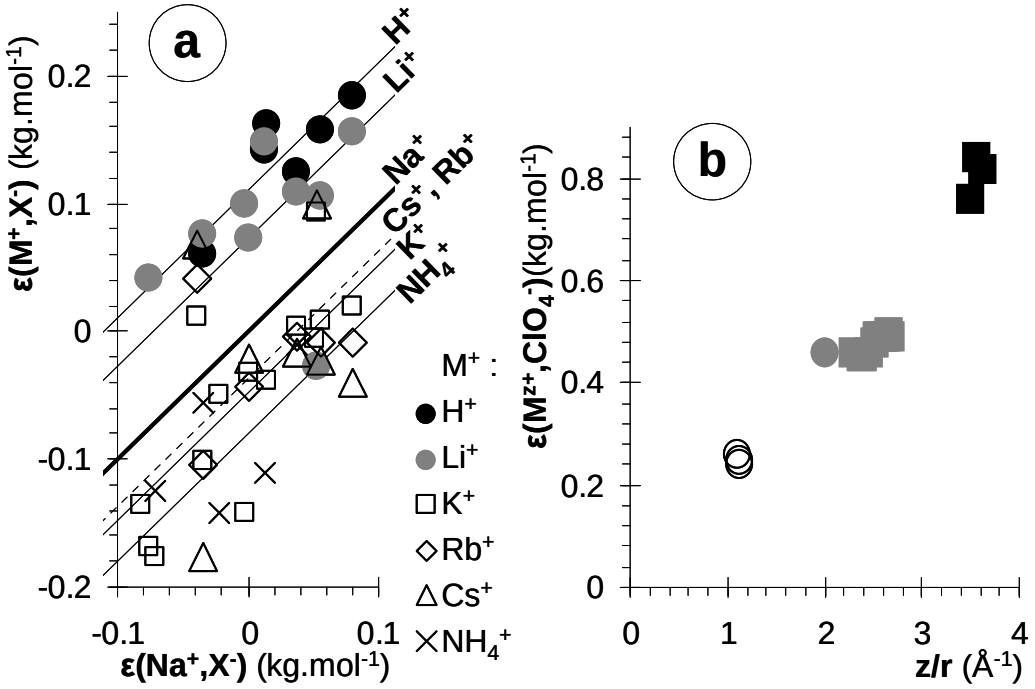

Figure 7. SIT ion pair interaction coefficients of hard cations

for (a) M^+ mono-cations (dilated scales) that are often used with various X^- mono-anions to maintain constant ionic strength, and (b) for the $M^{z+} = M^{3+}$ (grey squares), M^{4+} (black squares), AnO_2^+ (white circles) and AnO_2^{2+} (grey circles) actinide and analogous ions in ClO_4^- aqueous solutions.

3.4.2 Aqueous, Surfaces and Solid Solutions.

3.4.2.1 Introduction.

Up to now in this Chapter, we have outlined the aqueous chemistry of uranium, including the stabilities of its aqueous chemical species as given by equilibrium constants. We have also given, in Footnotes, details of the corresponding thermodynamics. The (very classical) way we have used thermodynamics is well adapted for chemical equilibria, especially at constant -or near constant- temperature and pressure for ideal -or near ideal- solutions. A similar approach can describe solid solutions [Vitorge 2008], which actually includes ionic exchanges of typically aqueous species with bulk or surfaces of other liquid or solid phases. This can be convenient to describe the solubility of uranium when controlled by mixtures or complicated natural

minerals. Even in very simple uranium solid compounds the stoichiometry of uranium can continuously vary. In this paragraph we essentially outline the thermodynamic basis of such well-known features in order to clarify and validate their use in typically assessments of radio-toxicities.

3.4.2.2 $U_{1-x}Np_xO_2$.

An example of a solid-solution matrix is UO_2(s) that can co-precipitate An^{4+}; the resulting An(IV)/U(IV) aqueous solubility ratio is classically found to be the same as the An(IV)/U(IV) ratio in the solid phase as typically measured for An = Np [Rai 2004]. This An(IV)/U(IV) ionic exchange behaviour provides evidence for a solid solution. It can dramatically decrease the Np(IV) aqueous concentration -when Np(IV) is at trace concentration- as compared to the solubility controlled by the pure (NpO_2(s)) compound. Since U^{4+} and Np^{4+} are ions of the same charge and similar sizes, their continuous ionic exchange in the solid is indeed not surprising. This mixture (or solid solution) is usually written $U_{1-x}Np_xO_2$(s). Adapting Lippmann's approach [Lippmann 1977, 1980] the thermodynamic modelling of the ionic exchange behaviour is obtained from the two

$$K_{An} = \frac{[An^{4+}(aq)]}{\left[\overline{An^{4+}}\right]\left[\overline{O^{2-}}\right][H^+(aq)]}$$

constants of the two

$$\overline{An^{4+}} + 2\ \overline{O^{2-}} + 4\ H^+(aq) \leftrightarrows An^{4+}(aq) + 2\ H_2O(\ell)$$

partition equilibria of An^{4+} between the aqueous solution and solid solution phases, for An = U and Np, where $\bar{i}$ is the concentration of Species i,[31] in the solid, classically mole fractions or other concentration units,[32] which gives the

$$K_{s,UO_2} = \frac{[U^{4+}(aq)]}{(1-x)[H^+(aq)]^4}$$

$$K_{s,NpO_2} = \frac{[Np^{4+}(aq)]}{x[H^+(aq)]^4}$$

set of Lippmann's equations, where K_{s,AnO_2} is the solubility product of the AnO_2(s) end-member pure compounds.[33]

---

[31] We write $U_{1-x}Np_xO_2(s) = (1-x)\ \overline{U^{4+}} + x\ \overline{Np^{4+}} + 2\ \overline{O^{2-}}$

[32] The mole fractions are $\chi_{U^{4+}} = (1-x)/3$, $\chi_{Np^{4+}} = x/3$ and $\chi_{O^{2-}} = 2/3$. We use the $\left[\overline{U^{4+}}\right] = 1-x$, $\left[\overline{Np^{4+}}\right] = x$, $\left[\overline{O^{2-}}\right] = 2$ equivalent concentration units.

[33] Using the units in Footnote [32] $K_U = \frac{[U^{4+}(aq)]}{4(1-x)[H^+(aq)]^4}$ and $K_{Np} = \frac{[Np^{4+}(aq)]}{4x[H^+(aq)]^4}$ Using this solid solution thermodynamic description for the AnO_2(s) end-member pure compounds [Michard 2002] it appears that (for x = 0) $4\ K_U = K_{s,UO_2}$ and (for

$$\frac{K_{s,NpO_2}}{K_{s,UO_2}} = \frac{[Np^{4+}(aq)](1-x)}{[U^{4+}(aq)]x} \frac{K_{s,NpO_2}}{K_{s,UO_2}} = K_{Np/U}$$

appears to be the constant of the

$$U^{4+}(aq) + \overline{Np^{4+}} \leftrightarrows Np^{4+}(aq) + \overline{U^{4+}}$$

ionic exchange equilibrium: the $[Np^{4+}(aq)]/[U^{4+}(aq)]$ ratio of aqueous concentrations is proportional to the $x/(1-x) = \left[\overline{Np^{4+}}\right]/\left[\overline{U^{4+}}\right] = \chi_{Np^{4+}} / \chi_{U^{4+}}$ ratio of mole fractions in the solid. Actually these ratios are virtually equal: $K_{Np/U} \approx 1$ since U and Np are chemical analogues -namely $K_{s,UO_2} \approx K_{s,NpO_2}$- as usual for actinides in the same oxidation state. The ionic exchange behaviour means that the aqueous concentration of the trace element (for example Np in the UO_2(s) matrix) can be much smaller than its solubility when controlled by pure compounds. Actually, the Np saturation index is exactly x,[34] which is indeed small, when Np is at trace concentration. This means that the solid solution is more stable than the pure compound when this thermodynamic description is valid.[35] $K_{Np/U}$ has been obtained by combining both (K_{An}) Lippmann's equations. Another combination of the (K_{An}) Lippmann's equations is the

$$K_{s,UO_2}^{1-x} K_{s,NpO_2}^{x} = \frac{[U^{4+}(aq)]^{1-x}[Np^{4+}(aq)]^{x}}{(1-x)^{1-x}\, x^{x}[H^{+}(aq)]^{4}}$$

formula extensively used by geochemists, sometimes attempting to add other empirical equations such as the stoichiometric dissolution approach. Another equation is indeed needed as can be deduced from Gibbs' phase rule, but the second equation is already known: the two Lippmann's equations suffice, or any of their combinations as typically for the ($K_{Np/U}$) ionic exchange equilibrium. The $K_{s,UO_2}^{1-x} K_{s,NpO_2}^{x}$ product is not constant (x varies): it is not the law of mass action constant for the

---

x = 1) 4 $K_{Np} = K_{s,NpO_2}$, where $K_{s,AnO_2} = \frac{[An^{4+}(aq)]_{AnO_2}}{[H^{+}(aq)]^4}$ is the solubility product of the AnO_2(s) end-member, and $[An^{4+}(aq)]_{AnO_2}$ is $[An^{4+}(aq)]$ when controlled by the AnO_2(s) end-member pure compound, namely for x = 0 (An = U) and x = 1 (An = Np) it appears that 4 $K_{An} = K_{s,AnO_2}$, it only means that the activities in the solids are their concentrations, and this is the definition of ideality.

[34] The saturation index is $s_{NpO_2(s)} = [Np]_{t,aq} / [Np(aq)]_{NpO_2}$, where $[Np]_{t,aq} = \alpha\, [Np^{4+}(aq)]$, $[Np(aq)]_{NpO_2} = \alpha_1\, [Np^{4+}(aq)]_1$, $\alpha = 1$ and $\alpha_1 = 1$ in acidic non-complexing conditions, in the other conditions they are the proportions of complexes -including hydrolysed species- of Np(IV); when the later are monomeric $\alpha = \alpha_1$ because they do not depend on Np concentration. In these conditions $s_{NpO_2(s)} = [Np^{4+}(aq)] / [Np^{4+}(aq)]_{NpO_2}$. From $K_{s,NpO_2} = [Np^{4+}(aq)] /(x\, [H^{+}(aq)]^4)$, and the $K_{s,NpO_2} = [Np^{4+}(aq)]_{NpO_2} / [H^{+}(aq)]^4$ definition given in Footnote [33] it appears that $x = [Np^{4+}(aq)] / [Np^{4+}(aq)]_{NpO_2} = s_{NpO_2(s)}$.

[35] This thermodynamic description essentially assumes that the law of mass action can be written with concentrations, or equivalently the solid solution is ideal. Intuitively this is possible only when ion exchange does not significantly disturb the matrix.

$$(1\text{-}x)\,\overline{U^{4+}} + x\,\overline{Np^{4+}} + 2\,\overline{O^{2-}} + 4\,H^+(aq) \rightleftarrows (1\text{-}x)U^{4+}(aq) + x\,Np^{4+}(aq) + 2\,H_2O(\ell)$$

dissolution equilibrium,[31] because x is written as a stoichiometric coefficient, while it has the meaning of concentration:[31,32] the thermodynamic demonstration of the law of mass action is valid for equilibria with constant stoichiometric coefficients, as pointed out by Lippmann. For this reason it is better re-demonstrating the law of mass action now with variable stoichiometric coefficients, to demonstrate directly the formula used by the geochemists. This essentially consists in adding a term corresponding to x as an advancement variable for a second equilibrium: the first equilibrium corresponds to the above dissolution equilibrium at constant x (stoichiometric dissolution), while the second equilibrium corresponds to the variation of the stoichiometry -with x- without dissolution: this is -of course- the above ionic exchange equilibrium.[36] This again demonstrates that two equilibria are needed to describe such systems. The two Lippman's equations can be combined to give the two ionic exchange and dissolution equations; conversely the two latter ones can be combined to give the Lippmann's equations: both descriptions are equivalent. It is the thermodynamic description of a solid solution.

Many ionic exchange equilibria are experimentally known on various supports (or matrix). The stoichiometric coefficients of the ionic exchange equilibrium can be interpreted as the derivatives of those for the dissolution reaction of the matrix.[36] Conversely integrating the stoichiometric coefficients of an ionic exchange equilibrium gives the stoichiometric coefficients of the dissolution / precipitation reaction for the matrix. Similarly, integrating -as a function of x- the law of mass action for an ionic exchange equilibrium gives the geochemists' equations for dissolutions / precipitations of the matrix.

3.4.2.3 UO_{2+y}.

Another example of a simple uranium compound with variable stoichiometries is $UO_{2+y}(s)$, which can be seen as a solid with the same matrix as that of $UO_2(s)$, where U

[36] $0 = dG = \sum_i \mu_i\, dn_i$ is used to demonstrate the law of mass action, where n_i is the number of moles of species i, and μ_i is its chemical potential. Substituting $dn_i = \nu_i\, d\xi$, gives $0 = \left(\sum_i \mu_i\, dn_i\right) d\xi$ where ξ is the advancement variable of the equilibrium, and substituting $\mu_i = \mu_i^0 + R\,T\,\ln[i]$ gives the law of mass action for the equilibrium with the constant ν_i stoichiometric coefficients: $0 = \Delta_r G + R\,T\,\ln K$, where $\Delta_r G = \sum_i \nu_i \mu_i^0$ and $K = \prod_i [i]^{\nu_i}$ For equilibrium $(1\text{-}x)\,\overline{U^{4+}} + x\,\overline{Np^{4+}} + 2\,\overline{O^{2-}} + 4\,H^+(aq) \leftrightarrows (1\text{-}x)U^{4+}(aq) + x\,Np^{4+}(aq) + 2\,H_2O(\ell)$ with variable stoichiometric coefficients $dn_i = \nu_i\, d\xi + \xi\, d\nu_i$ – not only $\nu_i\, d\xi$ when $d\nu_i \neq 0$-. The first $\sum_i \nu_i \mu_i$ term gives the $\frac{[U^{4+}(aq)]^{1-x}[Np^{4+}(aq)]^x}{4(1-x)^{1-x}\,x^x\,[H^+(aq)]^4}$ -non constant-quotient corresponding to the (-(1-x), -x, -2, -4, 1-x, x and 2) ν_i values, while the second term can be written $\xi\left(\sum_i \nu_i{}'\mu_i\right) dx$ where $\nu_i{}' = \frac{d\nu_i}{dx}$ namely the (+1, -1, 0, 0, -1, 1 and 0) $\nu i'$ values are calculated, and the $\sum_i \nu_i{}'\mu_i$ term appears to correspond to the $U^{4+}(aq) + \overline{Np^{4+}} \leftrightarrows Np^{4+}(aq) + \overline{U^{4+}}$ ionic exchange equilibrium.

is partially oxidised. Charge compensation is obtained by insertion of O^{2-} ions at least for small values of y, typically $y < 0.25$ corresponding to $U_4O_9(s)$ (= $4\ UO_{2+0.25}(s)$). Transuranians also form AnO_{2+y} solids, where the oxidation state of oxidised An is +5 (Pu) or +6 (U) [Conradson 2004].[37] U^{4+} is exchanged for UO_2^{2+} in the formation of $UO_{2+y}(s)$ from $UO_2(s)$. This exchange of ions with different charges can still be modelled with Lippmann's equations as typically proposed by Michard [Michard 2002]; however, exchanges of ions with different charges do not correspond to ideal solid solutions in most cases.[35] Special attention must be paid to the actual stoichiometry of such reactions, which actually reflect the particular structure that allows the exchange of ions with different charges without dramatic constraints on the matrix. This is also reflected in the concentration units within the solid phase. Formally $UO_{2+y} = (1-y)\ UO_2 + y\ UO_3$, but it should best be described with a larger elementary cell encompassing both end-members: $UO_2(s)$ and $U_4O_9(s)$ from $UO_2(s)$ with vacancies, filling the vacancies (with O^{2-}) without dramatic change in the geometry of the matrix. This can accommodate the $\overline{UO_2^{2+}}/\overline{U^{4+}}$ 1:1 ionic exchange. In that case the $[UO_2^{2+}(aq)]/[U^{4+}(aq)]$ ratio appears both in this ionic exchange and in the redox potential of the aqueous solution as given by the $E_{UO_2^{2+}(aq)/U^{4+}(aq)}$, the normal potential of the $UO_2^{2+}(aq)/U^{4+}(aq)$ redox couple and this gives quite a simple expression for the redox potential of the solution

$$E = E_{s_S} + \frac{E_N}{2a}(\lg 4 - \lg((1-a)^{1-a}\, a^a\, (2-a)^{2-a})) + \frac{E_N}{2}\lg\frac{y}{(1-y)(2-y)}$$

is obtained, where E_{s_S} is the potential of the solution equilibrated with both end-member pure solid compounds, not the solid solution. The E curve obtained (Figure 8) has the same shape as experimental measurements of P_{O_2}, the partial pressure of oxygen equilibrated with UO_{2+y} as measured at high temperature. The stoichometry used for the $\overline{UO_2^{2+}}/\overline{U^{4+}}$ 1:1 ionic exchange correspond to the

$$UO_{2+y} = (1-y)\overline{U^{4+}} + y\overline{UO_2^{2+}} + (2-y)\overline{O^{2-}}$$

decomposition, where the actual matrix is not straightforward to identify, in principle at least two types of $\overline{O^{2-}}$ are needed to describe such system, one type corresponding to the matrix, the other type filling vacancies to achieve charge balance in the course of the $\overline{UO_2^{2+}}/\overline{U^{4+}}$ 1:1 ionic exchange. This illustrates that different stoichiometric descriptions of the solid solution are possible, but they are not equivalent [Vitorge 2008]. Alternatively, one could typically consider a $2\overline{UO_2^{2+}}/\overline{U^{4+}}$ 2:1 ionic exchange, where $\overline{O^{2-}}$ can now be

[37] If PaO_{2+y} is formed, and if oxidised Pa is in the form of $\overline{PaO_2^+}$ this might be used –together with thermodynamic cycles similar as those in Ref. [Vitorge 2003]- to estimate the thermodynamic stability of $PaO_2^+(aq)$ beside mass spectrometry studies of the Pa(V) hydration or dehydration.

identified to the matrix, or many other possibilities: in principle the correct one is given by experimental observations.

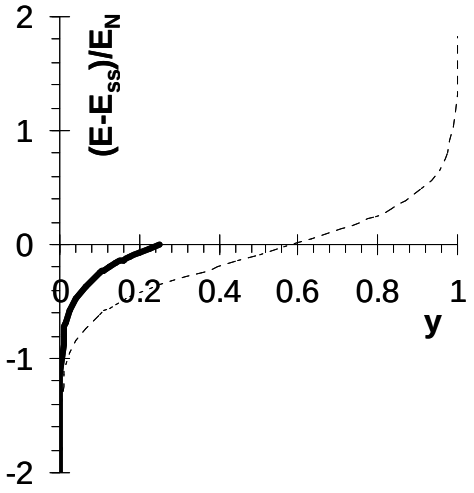

Figure 8. Redox potential controled by a solid solution.

E is the redox potential of the aqueous solution equilibrated with the UO_{2+y} solid solution of UO_2(s) and U_4O_9(s) end-members (thick curve): $0 \le y \le 0.25$; for $y > 0.25$ another solid phase (not taken into account) is stable. E_{ss} (noted E_{s_s} in the text) is the redox potential of an aqueous solution equilibrated with both UO_2(s) and U_4O_9(s) end-members pure compounds -hence when no solid solution is formed-, E_{ss} depends only on pH. The dashed line is the curve if UO_3(s) were the end-member instead of U_4O_9(s).

Dramatic changes are predicted in E, only when U(VI) is at trace concentrations inside the solid solutions. When the solubility products of the end-members are known, this gives the value E_{s_S}: measured E should be about the value of E_{s_S} Conversely, this E_{s_S} numerical value can allow to detect a solid solution, despite quite similar shapes of the curves as in are expected in homogeneous aqueous solutions or after the precipitation of a single end-member.

4. MOLECULAR MODELLING OF SPECIES CONTAINING THE URANYL ION.

4.1 INTRODUCTION

The aqueous chemistry of uranium is quite well known and understood (see Section 3). Nevertheless, the thermodynamic stabilities of some important aqueous uranium complexes and hydroxides need to be confirmed. In this section we outline a few examples using molecular modelling to address such questions. The thermodynamic stabilities of chemical species are given by the $\Delta_r G$ Gibb's energies of formation reactions or of any well chosen equilibria at given temperature and pressure. Unfortunately, calculating $\Delta_r G$ is not the most straightforward use of molecular modelling, and in most cases the accuracy is not sufficient for reactions in liquid water.

Conversely, molecular modelling is often appropriates for obtaining geometries, which is often useful to understand stabilities. Quantum mechanics is also needed to understand covalent bonding: UO_2^{2+} is typically a linear covalent molecular ion. Many molecular modelling methods are currently used -based on classical or quantum mechanics- giving optimized structures or simulating the dynamics of the system. Quantum calculations essentially describe electrons, while classical molecular models usually describe the atoms typically with given charges and eventually polarizabilities, but without explicit description of their electronic origins.[38] For this reason, classical -*i.e. no explicitly quantum*- molecular modelling is not specially appropriate to simulate the formation of covalent bonds. Furthermore classical models require empirical potentials to account for the essentially quantum interactions:[39] these potentials are nowadays parameterized with quantum calculations, which -in this way- are used in most molecular modelling methods.

Quantum calculations are easier with closed-shell electronic structures, so for this reason it is logical to start the molecular modelling studies of uranium with U(VI), while other oxidation states are rather studied on chemical analogues (see Section 3.1.1). The geometries of the U(VI) species in liquid water and in many other media are well known: they are usually built on the linear UO_2^{2+} uranyl molecular dication. We shall report molecular modelling studies of its hydration. It is also interesting to check that UO_2^{2+} is the most stable isomer in aqueous solutions –to check first the quantum calculations and their interpretation.

In a first step we here report quantum calculation results of $UO_2(H_2O)_i^{2+}$ species built by adding H_2O molecules one by one to UO_2^{2+} up to the saturation of its first hydration layer in the gas phase (Section 4.2) in an aim to start modelling the aqueous chemistry of U(VI) or at least its hydration.[5] It appears that the hydration of $UO_2(OH)_j(H_2O)_i^{(2-j)+}$ oxo-hydroxo species of UO_2^{2+} can be calculated in the same way, also corresponding to its hydrolysis (Section 4.2).[13] Such quantum calculations of isolated ions in the gas phase are classically compared to mass spectrometry experiments for validating the quantum method. This is done here by using published mass spectrometry results for the $UO_2(OH)(H_2O)_i^+$ mono-cation of U(VI) (Section 4.3). These hydration and hydrolysis quantitative studies, together with qualitative discussions give insight in the reasons of the stability of the UO_2^{2+} uranyl ion (Section 4.4). A single explicit hydration layer is not always sufficient to obtain the exact geometry and other physical parameters for the hydration sphere of UO_2^{2+}, while recent studies showed that an explicit second hydration

[38] The explicit description of polarization is needed for modelling highly charged ions in water, including La^{3+} [Duvail 2007] and UO_2^{2+} [Clavaguéra 2003].[39]

[39] Anions and cations would stick together if modelled by only classical electrostatics. Their short-range repulsions are of quantum origin. When this repulsion is modelled with empirical pair-interaction model potentials, these potentials also account for all the other interactions that are not correctly described in the classical electrostatic model. However, some of the actual interactions –among which polarization- are not purely pair interactions.

layer can give the correct results for the hydration of UO_2^{2+} and -at least- some of its complexes (Section 4.5). To our knowledge, constructing such a model second hydration sphere -and proposing they really make sense- was first published for UO_2^{2+}. First-principle molecular dynamics studies of the hydration and the first hydrolysis of UO_2^{2+} have been recently published (Section 4.6). Finally, we report some results on $U(OH)_4$ and analogous species (Section 4.7).

4.2 Hydration and Hydrolysis of Uranyl in the Gas Phase.

The simplest idea for modelling the hydration of UO_2^{2+} is to add water molecules one by one -hence in gas phase. A regular increase in the energy of the reactions is observed (Figure 9). As expected, a maximum number of water molecules is reached, when the first coordination layer is full: 5 water molecules consistent with experimental results in liquid water. Adding a 6th H_2O actually results in geometric rearrangement on optimisation: finally there are only 4 water molecules in the first hydration layer, while the 2 other water molecules are between the 1st and 2nd hydration layers. The $UO_2(H_2O)_5^{2+}$ stoichiometry appears to predominate both in the gas and aqueous phases at the $H_2O(g)$ / $H_2O(\ell)$ limit characterised by $P_{H_2O,l/g}$, the liquid-gas equilibrium water partial pressure (Figure 9). This is the result of several effects that cancel out; but this is not fortuitous. The first hydration layer is in the equatorial plane of linear UO_2^{2+}. The Gibb's energies of the successive hydration reactions can be used to plot the predominance diagram as a function of the activity of the exchange species, here H_2O (vertical scale in Figure 9) whose activity is classically P_{H_2O}: i, the coordination number in $UO_2(H_2O)_i^{2+}$ increases with P_{H_2O}.

It appears that obtaining $UO_2(H_2O)_i^{2+}$ in equilibrium conditions requires unrealistically low P_{H_2O} values for i = 0, 1 and 2 as deduced from the $\Delta_r G$ values (minus a few tens of kJ.mol^{-1}): UO_2^{2+} is hydrated at once by any trace of water. Similar hydrations have been constructed for other U(VI) species of different charges obtained by adding H^+ to an O_{yl} of UO_2^{2+} or suppressing H^+ from an equatorial water molecule of the first hydration layer, corresponding to base/acid -or equivalently protonation/hydrolysis- reactions. Each hydrolysis (suppressing an H^+) decreases the charge by one, which results in less easily hydrated species. Now a regular increase in the energies of the reactions is again observed for the successive hydrolysis of UO_2^{2+}. Surprisingly, this is still the case, when starting from $UOOH^{3+}$, a UO_2^{2+} protonated species: UO_2^{2+} does not specially appear to have a much bigger predominance domain towards acid base reactions. The computed structure of $UOOH^{3+}$ is difficult to obtain, and the added H^+ is not strongly bonded -as reflected by the (106 pm) relatively long UO_{yl}-H distance. This suggests that on hydration the linear $UOOH^{3+}$ structure might rearrange to a more stable trication as typically $U(OH)_3^{3+}$.[13] Such study would require many calculations: we did not further study the hydrations of U(VI) trications, because no U(VI) trication has ever been detected

-even in very acidic conditions- to our knowledge.

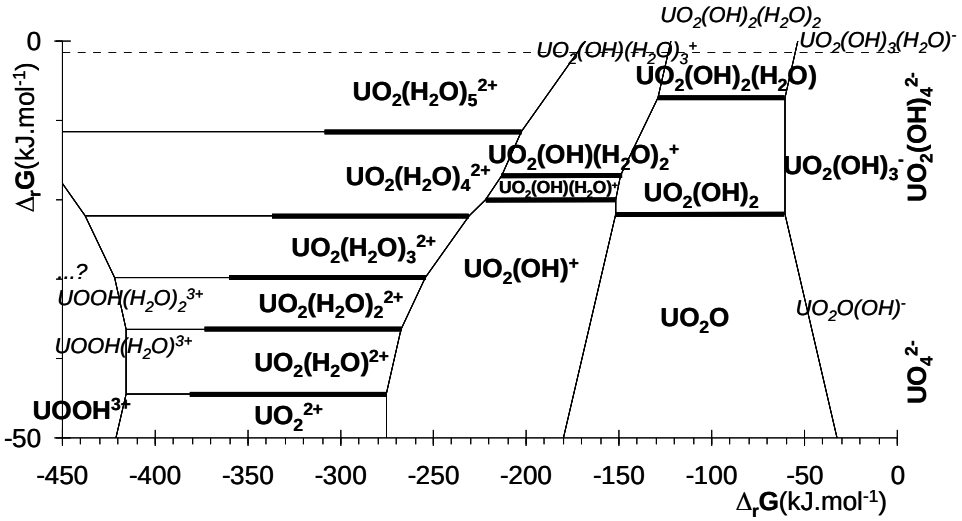

Figure 9. Calculated energies of hydration and hydrolysis for UO_2^{2+} in the gas phase.

Each horizontal line corresponds to the energy change (vertical scale) for the successive hydration reactions. As in the Pourbaix diagrams (Figure 2) the $\Delta_r G$ scale can be associated with the corresponding equilibrium constant and the half-reaction point (not shown on this figure): $P_{H_2O,1/2}$, the H_2O partial pressure at the half-reaction point for the hydration reactions. For this reason the horizontal lines are also the boundaries of the predominance domains for the species written on the figure as a function of P_{H_2O}. Similarly the horizontal scale is proportional to pH for hydrolysis reactions. The stabilities of the italicised species have not been calculated. The upper limit of $\Delta_r G$ (dashed line) corresponds to $P_{H_2O,\ell/g}$, the liquid-gas equilibrium water partial pressure at 25°C and 1 atm, *i.e.* the maximum P_{H_2O} value in the gas phase, where $H_2O(g)$ is condensed into $H_2O(\ell)$.

In conclusion, as expected and consistently with published similar studies for many cations, a regular increase is observed for the energy changes of the successive additions of H_2O on UO_2^{2+} in the gas phase up to the saturation of the first hydration layer, where the (5) same coordination number as in liquid water is found.[40] This is not completely fortuitous despite one hydration layer is not completely satisfactory for modelling hydration in liquid water (Section 4.5.2). Regular energy changes are also found for the successive hydrolysis of hydrated U(VI) ions in the gas phase; while the experimental hydrolysis constants indicate it is not really the case in liquid water: this suggests that modelling should take into account details of the hydrations of reactants and products. We did not find (Figure 9) that the great stability of UO_2^{2+} is associated with a bigger size for its predominance domain (Section 4.4).

[40] The (CN) coordination numbers in the gas phase depend on P_{H_2O}: CN increases with P_{H_2O} up to a CN_{max} maximum value when the first hydration layer is saturated (CN is limited by steric repulsions) if $P_{H_2O,1/2,CN_{max}}$ is less than $P_{H_2O,\ell/g}$ (Figure 9).[41] In this case CN(g), "the coordination number in the gas phase" can be defined as $CN(g) = CN_{max}$. Otherwise the meaning of CN(g) might not be clear.

4.3 Comparison of Quantum Calculations with Mass Spectrometry Experiments.

Presenting the energy results as a Pourbaix-like predominance diagram (Figure 9), gives $P_{H_2O,1/2,i}$, the water partial pressure half-reaction point for adding the i^{th} water molecules to U(VI) species in the gas phase.[41] This can be compared with experimental results for the -relatively small- range of (P_{H_2O}) water partial pressure values that can be obtained experimentally at reasonable cost. Indeed, quantum calculations are classically validated by mass spectrometry measurements. Gresham *et al.* studied the formation of adduct ions consisting of U(VI) dioxo monocations -among other uranium mono-cations- and water using an ion trap secondary ion mass spectrometer (IT-SIMS). The U(IV) ion $UO(OH)^+$ was produced by bombarding the surface of solid UO_3 using molecular primary ions, and the U(VI) ion $UO_2(OH)^+$ was generated by O_2 oxidation of $UO(OH)^+$ in the gas phase. The resulting U(VI) ion $UO_2(OH)^+$ was further hydrated at controlled P_{H_2O} = 1.8 10^{-9} atm: it added up to 3 water molecules. The authors fit kinetic models to the time-dependent mass spectral data to estimate reaction rates and rate constants. [$UO(OH)^+$] decreased with the reaction time, giving $UO_2(OH)^+$, whose concentration increased only at the shortest times, then being hydrated: its maximum concentration was observed after 0.5 s. The concentrations of $UO_2(OH)(H_2O)^+$ and $UO_2OH(H_2O)_2^+$ were small during all the experiments, they were stable or slightly decreasing at the end of the experiments: their maximum concentrations -if any- were observed at about 1 s and 1.5 s. The concentration of only $UO_2OH(H_2O)_3^+$ clearly increased during all the experiments, and it was the major mono-cation product after about 1.2 second. The authors concluded that stabilities of the hydrate complexes $UO_2OH(H_2O)_i^+$ increase with increasing i, until the optimum number of ligands is achieved. The maximum coordination number of 4 they observed for hydrated $UO_2(OH)^+$ in the gas phase is the same as that we proposed from quantum calculations for $UO_2(OH)^+$ in liquid water [Siboulet 2006, 2008]. However, the activity of water is different in liquid water and in the gas phase: i is expected to increase with P_{H_2O} in equilibrium conditions. $P_{H_2O,1/2,i}$ for the reaction

$$UO_2OH(H_2O)_{i-1}^+ + H_2O \rightarrow UO_2OH(H_2O)_i^+$$

is related to the Gibb's energy change -or equivalently K_i, the constant of the corresponding equilibrium-[17] that we calculated from the $k_{f,i}$ / $k_{r,i}$ (= K_i) ratio of the forward / reverse kinetic constants assuming thermalisation was achieved, at least for the longer reaction times. We obtained 1.0 10^{-9} atm, 3.3 10^{-10} atm and 1.8 10^{-10} atm for i = 1, 2 and 3, respectively. According to these $P_{H_2O,1/2,i}$ values deduced from mass spectrometry, $UO_2OH(H_2O)_3^+$ would be formed at lower P_{H_2O} than the lower hydrates: this is not realistic, showing that our thermodynamic calculation are meaningless, certainly

[41] $P_{H_2O,1/2,i}$ for the exchange of $H_2O(g)$ is defined in the same way as $pH_{1/2,i}$ for the exchange of H^+.[16]

because thermalisation was not achieved -at least- in the early stages of the experiments. For this reason we focus only on the species formed at the longer times corresponding to $P_{H_2O,1/2,3} = 1.8\ 10^{-10}$ atm. It is consistent with the above qualitative observations: the $1.8\ 10^{-9}$ atm experimental P_{H_2O} in the mass spectrometer was an order of magnitude higher than $P_{H_2O,1/2,3}$, corresponding to 90 % of $UO_2OH(H_2O)_3^+$ in equilibrium conditions, which was not reached within the time of the experiment: only 40 % of $UO_2OH(H_2O)_3^+$ at the end of the experiments, and its concentration did not reach a plateau, it increased all the time.

$P_{H_2O,1/2,3} = 1.8\ 10^{-10}$ atm calculated from the mass spectrometry kinetic data is 4.5 times the $P_{H_2O,1/2,3} = 4.0\ 10^{-11}$ atm value we estimated from quantum calculations,[5] which also confirms that the $P_{H_2O,1/2,i}$ values are much smaller for i = 1 and 2. This factor of 4.5 time difference is significant as compared to the accuracy expected for P_{H_2O} measurements, but it corresponds to only 4 kJ.mol^{-1} in $\Delta_r G_3$, a value smaller than the accuracy of the quantum calculations, and certainly within the uncertainty of the thermodynamic interpretation of the mass spectrometry kinetic results, where temperature and thermalisation are at the origin of important uncertainties for the kinetic and thermodynamic interpretations.

As a conclusion, our quantum calculations are consistent with the published mass spectrometry results; but the comparison is hampered by substantial uncertainty due to our thermodynamic interpretation of the mass spectrometry results.

4.4 Why is Uranyl so Stable?

A first idea to estimate the stability of UO_2^{2+} is to compare its thermodynamic stability to that of the other hydrated U(VI) oxo-hydroxo-species. Thermodynamic stabilities are illustrated in predominance diagrams: the predominance domain of UO_2^{2+} or of its hydrated species does not appear to be much larger than that of the other hydrated U(VI) oxo-hydroxo-species (Figure 9). Actually the UO_2^{2+} geometry still exists in most of the other species written on the predominance diagram. In all these species the linear or quasi-linear UO_2^{2+} geometry is virtually unchanged on adding H_2O and HO^- ligands in its equatorial plane: UO_2^{2+} should rather be considered to be in the whole predominance diagram, when considering this molecular (sub)-unit. For this reason the great stability of UO_2^{2+} should not be found in the energies changes involving UO_2^{2+}, at the origin of the diagram. The great stability of UO_2^{2+} is rather reflected in the quasi-absence of geometrical changes on adding the ligands. This very stable geometry is due to the two covalent U≡O_{yl} uranyl triple bonds. Indeed the covalent uranyl dication is found in most U(VI) complexes and compounds. It is tempting to propose that this is originated in the equatorial hard character of U: the equatorial ligands would not form covalent bonds with U, hence not altering the electronic configuration that gives the two U≡O_{yl} triple covalent bonds. Unfortunately; such explanation is not consistent with quantum calculations for the HO^- ligand.[5,6] Population analyses rather suggest U-$(OH)_{eq}$ covalent

bonding. The H_2O and -to a larger extend- the HO^- equatorial ligand lengthen the $U{\equiv}O_{yl}$ distance, showing a weakening of the $U{\equiv}O_{yl}$ bonds, as also reflected in the charge transfer within UO_2 on adding equatorial ligands. Nevertheless, all these effects are not sufficient to destabilize the uranyl ion. Conversely it can be destabilized by F^- ligands in UF_6.

Interestingly, recent quantum studies allow comparisons with isolelectronic PaO_2^+ and other Pa(V) ions [Siboulet 2008, Toraishi 2006]. The calculated negative charges of the O_{yl} atoms increase *-i.e.* become less negative- in the $^{91}PaO_2^+ < {}^{92}UO_2^+ < {}^{93}NpO_2^+$ non-isoelectronic series [Siboulet 2008].[42] This can be interpreted as reflecting more difficult protonation of O_{yl} from Pa to Np, more electron transfer from the O_{yl} lone pairs and consequently stronger $An{\equiv}O_{yl}$ covalent bonds. PaO_2^+ and UO_2^{2+} have closed-shell isoelectronic structures, and the extra electrons in UO_2^+ and NpO_2^+ (as compared to PaO_2^+) do not participate in the bonding. This is consistent with the strong $U{\equiv}O_{yl}$ bonds in UO_2^{2+}. Hydrated PaO_2^+ species can be calculated, but they do not correspond to the aqueous Pa(V) mono-cation. PaO_2^+ is protonated in liquid water, and this protonation can lead to the hydrated $PaOOH^{2+}$ protonated protactinyl dication, *i.e.* a dication that can still be described as built on the linear $O{\equiv}Pa{\equiv}O$ skeleton, actually similar to the $UOOH^{3+}$ geometry we calculated. This suggested that we should construct the Pa(V) mono-cation from the $PaOOH^{2+}$ or -why not- the $PaOHOH^{3+}$ linear protonated protactinyl skeletons by adding HO^- equatorial ligands. Doing this, the $PaOHOH(OH)_2^+$ di-hydrolysed di-protonated linear protactinyl cation rearranged into tetrahedral $Pa(OH)_4^+$ that might very well be the most stable Pa(V) mono-cation in liquid water. The electronic configuration of $Pa(OH)_{4,Td}^+$ cannot be the same as in the PaO_2^+ actinyl species: the geometries are too different. Furthermore, the change from bent (ThO_2) to linear (PaO_2^+ and UO_2^{2+}) geometries is attributed to the inversion of the 6d and 5f energy levels across the $^{90}ThO_2$, $^{91}PaO_2^+$ and $^{92}UO_2^+$ series of isoelectronic actinide ions: the linear actinyl geometry is due to the f-characters of the $An{\equiv}O_{yl}$ triple bonds for An = Pa and U. Now this f-character is more important for U than Pa. This certainly means that it is more difficult to change the energy order of the valence electronic levels involved in the uranyl skeleton. However, we found that UO_4^{2-} also rearranged into a tetrahedral geometry;[5] but this species is not stable on hydration (Figure 9). Conversely, the $U(OH)_4^{2+}$ di-cation is actually di-hydrolysed di-protonated $U(OH)_2(OH)_2^{2+}$, not $U(OH)_{4,Td}^{2+}$, the U-OH distance are virtually the same, but the O-U-O angles are clearly not 109° (Table 1).

As a conclusion, the great stability of the linear UO_2^{2+} uranyl ion is simply due to its electronic configuration, which is not substantially altered on adding ligands, even when the bonding with equatorial ligands has some covalent character. Conversely, the actinyl

[42] Quantum calculations were also[5] done using the ADF program to incorporate spin-orbit coupling [Baerends 2006, Fonseca Guerra 1998, te Velde 2001]. Details of the calculations are described in Ref. [Siboulet 2008].

geometry can be destabilized by the very electronegative F^- or O^{2-} ligands (while HO^- induces some charge transfer, but without dramatic change in the electronic configuration of the UO_2^{2+} uranyl ion skeleton), or when the f-actinyl character might be less strong as recently explained for isoelectronic Pa(V).

4.5 THE TWO-SPHERE CLUSTER METHOD

4.5.1 Introduction

The two-sphere cluster method was recently developed to study the hydration of UO_2^{2+}. It gave surprisingly accurate results. We first describe these results (Section 4.5.2). It was then tempting to use the method for the hydration of other aqueous species. This was done for understanding Pa(V) aqueous chemistry in non-complexing aqueous solutions as recently published [Siboulet 2008], and for several complexes of U(VI) among which fluoride (Section 4.5.3) and acetate (Section 4.5.4) complexes described below.

4.5.2 Hydration of Uranyl

Several modelling techniques can be used as typically static quantum calculations in gas phase or simulating the bulk solution with models based on a polarisable dielectric continuum [Cramer 1999, Tomasi 1994, 2002], or molecular dynamics. Such theoretical chemical calculations have been used to study the hydration of the UO_2^{2+} uranyl ion [Bühl 2005, Bühl 2006, Cao 2005, Clavaguéra-Sarrio 2003, Gutowski 2006, Hay 2000, Rotzinger 2007, Shamov 2005, Siboulet 2006, Spencer 1999, Vallet Wahlgren Schimmelpfennig Moll 2001, Vallet Wahlgren Schimmelpfennig Szabó 2001, Wahlgren 1999]. The results obtained for the $U{\equiv}O_{yl}$ bond lengths are unsatisfactory, when not any explicit H_2O is included in the geometric model even with COSMO, a polarisable dielectric continuum formalism. Significant improvement is obtained if the first hydration shell is treated explicitly by quantum mechanics, and using COSMO [Fuchs 2002, Moskaleva 2004]. This confirms that the -at least- first hydration layer is essential to model $UO_2^{2+}(aq)$ as observed for the hydration of other cations.[43] The experimental cation-water distances are usually not exactly reproduced in optimized geometries for clusters consisting of a single cation and a single hydration sphere. Several authors suggested it was originated in the influence of bulk or second sphere water [Clavaguéra-Sarrio 2003, Gutowski 2006, Ikeda 2008, Shamov 2005, Siboulet 2006, Vallet Wahlgren Schimmelpfennig Szabó 2001]. Besides the static optimizations of two hydration sphere clusters we report in the present section, this was recently evidenced by Ikeda *et al.* [Ikeda 2008], who concluded their molecular dynamics simulations gave $U\text{-}O_{eq}$ distances in agreement with EXAFS results, while it was not the case for their -actually one hydration layer- static DFT results.

[43] $M^{z+}(aq)$ aqueous cation can best be written $M(H_2O)_n^{z+}(aq)$ where n is typically the mean number of H_2O in the first hydration layer, or the n value for the predominant isomer.

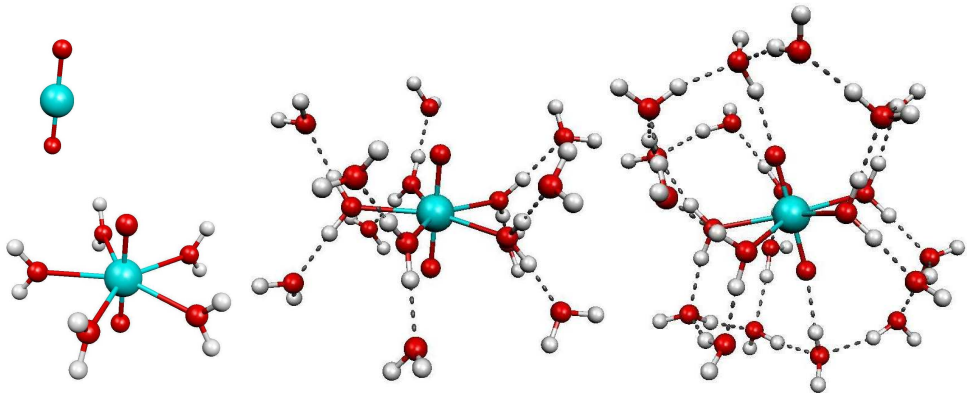

Figure 10. Geometrical models for the hydration of UO_2^{2+}

with 1 and 2 hydration layers, and with 2 hydration layers with apical H_2O water molecules (from left to right). U is blue, O red and H white [Siboulet 2006]. The figure is drawn with MOLEKEL [Portmann 2000, Flükiger 2002].

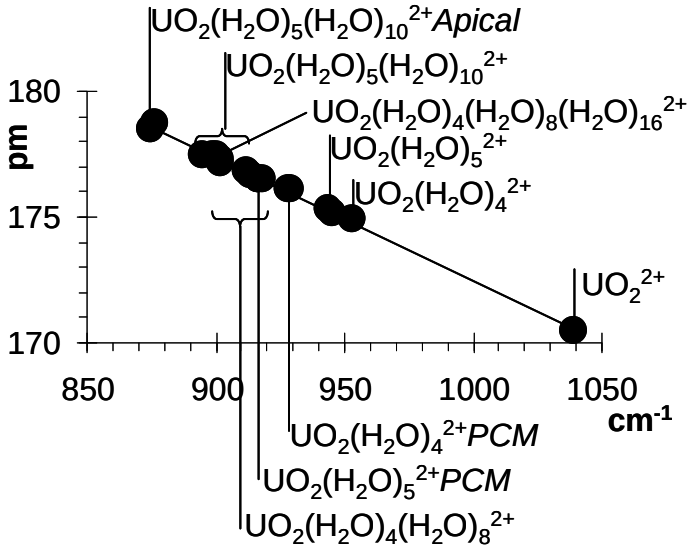

Figure 11. Correlation between calculated U≡O_{yl} uranyl bond lengths and Raman frequencies

for models of UO_2^{2+} with 0, 1 or 2 hydration layers, and, in some cases, apical water molecules or a dielectric continuum model (PCM) [Siboulet 2006].

They proposed it was originated in the dependence on the second coordination sphere model, citing Ref. [Siboulet 2006] that we will describe in this section. The most popular method to model hydration with quantum mechanics is to put the ion or the cluster in a cavity of a dielectric continuum. This indeed improves the model, demonstrating the non-negligible effect of the bulk water. It is also tempting to add explicit water molecules beyond the first hydration sphere; but the geometry of such a cluster is quite difficult to optimize, because the second-sphere water molecules are weakly bonded, resulting in a potential energy surface that is too flat for straightforward

geometry optimisation. It was indeed proposed that the H_2O molecules in the second sphere can also have some importance; for this reason molecular dynamics simulations was used with periodic conditions -hence for infinite systems- rather than "optimizations of realistically large [two hydration sphere] clusters [which] are a formidable task due to the myriads of local minima that can be involved" [Bühl Kabrede 2006]. Nevertheless, two-sphere model clusters were used in recent studies, giving surprisingly accurate data for the hydration of UO_2^{2+} in three independent studies [Gutowski 2006, Shamov 2005, Siboulet 2006], probably because the planar equatorial coordination geometry in UO_2^{2+} is quite simple. Some of these published two-sphere clusters have geometries with typically one water molecule H-bonded to each H atom of each water molecule of the first hydration layers (Figure 10). Similar results (not shown) were obtained with the O atoms of the second-sphere water molecules bridging two H atoms of two different first-sphere water molecules [Shamov 2005].

Such model geometries enable one to put a water molecule in apical position -*i.e.* its H atom close to the O_{yl} atom. The optimized UO_{yl}-HOH apical distance is 192 pm, a little smaller than obtained by a CPMD simulation (see Section 4.6).

The geometries of several models of hydrated UO_2^{2+} have been optimized, showing small differences between several geometrical and physical parameters of UO_2^{2+} such as $d_{U\equiv O_{yl}}$, its bond length, v_{UO_2}, its Raman frequencies, q_U and $q_{O_{yl}}$, the charges of its atom, and its first and second sphere coordination numbers: $d_{U\equiv O_{yl}}$, v_{UO_2} and $q_{O_{yl}}$ appear to be linearly correlated. One of these correlations is illustrated in Figure 11. $d_{U\equiv O_{yl}}$ increases on adding the first coordination layer to UO_2^{2+}.

This increase is slightly larger for the coordination number of 5 (as compared to 4), and slightly larger with the continuum model; but explicit second spheres have a greater effect. The biggest $d_{U\equiv O_{yl}}$ is found with apical water, while adding an explicit third sphere has virtually no effect. The apical two-sphere model best reproduces the experimental EXAFS $d_{U\equiv O_{yl}}$ values: the agreement is virtually within the uncertainties of the experimental values [Siboulet 2006]. The lengthening of $d_{U\equiv O_{yl}}$ can be interpreted as reflecting the diminution of the $U\equiv O_{yl}$ bond strength, consistent with the decrease of v_{UO_2}. This also corresponds to more negative $q_{O_{yl}}$ values, still consistent with the diminution of the $U\equiv O_{yl}$ bond strength induced by electron transfer from covalent bond to the O_{yl} electronic lone pair, which also facilitates apical H-bonding.

As a conclusion, even though only model geometries -not the true optimized geometries if any- are used, the two-sphere model cluster approach gives insight into the effects of the second sphere on several physical and geometric parameters, and it allows a discussion of the existence -or not- of apical water. As an example and for practical applications $d_{U\equiv O_w}$, the distance between U and the equatorial O atom of H_2O is overestimated by about 8 pm for the single coordination layer geometry. Dielectric continuum models can correct most of it. Now the apical two-sphere models give $d_{U\equiv O_w}$ = 236 pm and 242 pm for coordination numbers 4 and 5, respectively, while the experimental value is 242 pm, hence in agreement with the coordination number of 5,

which is certainly the best accepted value in the literature. It is tempting to use such methodology to help interpreting experimental results based on the cation-ligand distances, since it is often difficult to determine the coordination number from experimental results for species dissolved in liquid water, while the cation-ligand distance can be accurately given both by experiments and molecular modelling. The later can thus be used to propose the geometries that best model the experimental distances. This should give the stoichiometry. Similarly, when the U-OH_2 computed distance is larger than in all the known aqueous complexes this suggests that the last added H_2O molecule will in fact go to the bulk water in equilibrium conditions. Indeed, the U-OH_2 distance in the equatorial plane of UO_2^{2+} is always 240 pm within a few pm in most published structures, as pointed out in Ref. [Siboulet 2008].

4.5.3 Fluoride Complexes of Uranyl

The F^- ion can destroy UO_2^{2+} giving UF_6(g); but for moderate F^- aqueous concentrations $UO_2F_i^{(2-i)+}$ complexes are formed: $\lg K_i^0$ = 5.16 ± 0.06, 3.67 ± 0.08 and 2.17 ± 0.10 for the successive complexation constants with i = 1, 2 and 3 respectively as proposed in the updated NEA-TDB review, essentially based on the work of Ref. [Ferri 1993]. These values are consistent with the original selection [Grenthe 1992]. Values are proposed for higher complexes (i = 3 and 4) but we calculated they had nearly negligible effects on the measurements used to determined their values.

Successive additions of F^- on UO_2^{2+} induce a -12 cm^{-1} shift in the Raman vibration of UO_2^{2+} per added F^- [Nguyen-Trung 1992]. Our quantum calculations give -54 cm^{-1} and -13 cm^{-1} with 1 and 2 hydration layers respectively. This again illustrates the role of the second hydration layer, which is here needed to model Raman shifts quantitatively.

4.5.4 *The Aqueous Mono-Acetate Complex of Uran*yl

We have optimized[5] the geometries of $UO_2(CH_3COO)$ with several water molecules added in the equatorial first hydration layer of U, then adding further water molecules. With only bidentate CH_3COO^{2-} there is sufficient room for 2 to 4 extra water molecules in the equatorial first hydration layer, since the equatorial coordination number of UO_2^{2+} is 5±1 in most published structures. The highest coordination numbers are expected with multidentate ligands (as typically in Figure 5), when the donor atoms of the same molecule are held quite close together.

For this reason we compared structures with 3 and 4 equatorial first-layer water molecules. The U-O_{eq} distances for the different types of equatorial O_{eq} atoms -namely O_{water} and $O_{acetate}$- are close enough to give a single peak in the Fourier transform of the experimental EXAFS signal. Such U-O_{eq} mean distances have recently been measured at 241 pm [Jiang 2002]. 238 pm was obtained in Ref. [Schlosser 2006] by averaging 241 pm with older determinations [Allen 1997, Moll 2003]. The U-O_{eq} mean distances are 239 and 253 pm, respectively, for typical model two-sphere clusters with 3 and 4 water molecules respectively: only the (239 pm) geometry optimized with the 3 water molecules is consistent with the 241 pm or 238 pm experimental value. Similarly a

published study obtained 237.7 pm and 242.1 pm for the U-$O_{acetate}$ and U-O_{water} distances, respectively, giving the 240 pm mean value for a one-sphere model with PCM [Schlosser 2006].

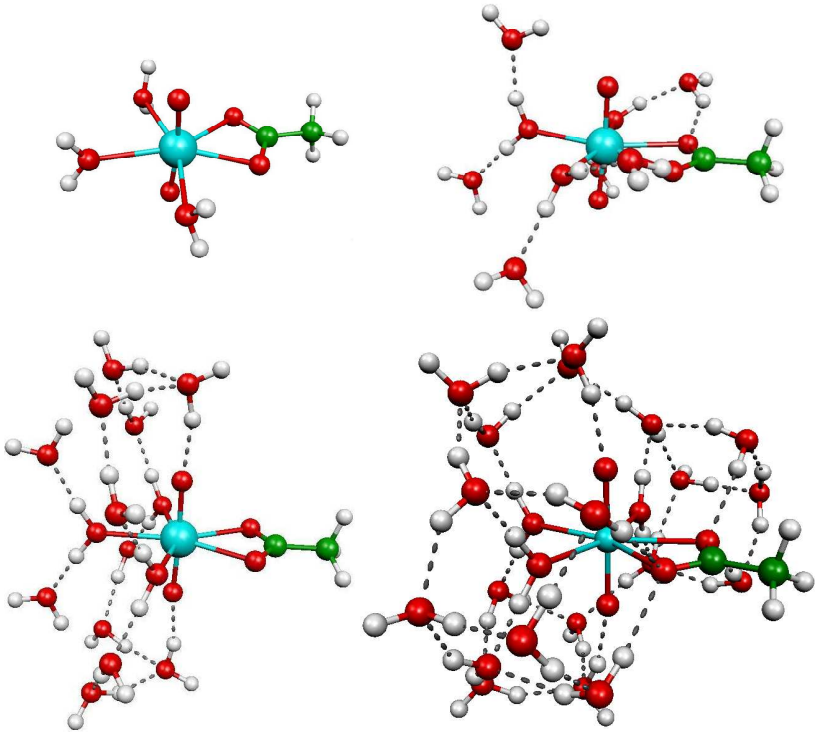

Figure 12. $UO_2(CH_3COO)$ hydrated clusters.

From left to right in the first then second line: c, $c(H_2O)_6$, $c(H_2O)_6(H_2O)_6$ and $c(H_2O)_6(H_2O)_6(H_2O)_8$, where c = $UO_2(CH_3COO)(H_2O)_3$, and $c(H_2O)_i(H_2O)_j(H_2O)_k$.is $UO_2(CH_3COO)$ with 3 H_2O molecules in the first hydration layer of U, in the equatorial plan of UO_2^{2+}, i (= 0 or 6) H_2O molecules in the second hydration layer H-bonded on the 3 previous ones, j (= 0 or 6) H_2O molecules holding one apical H_2O on each O_{yl}, and k (= 0 or 8) H_2O molecules H bonded on the O_{ac} atoms of CH_3COO^{2-}. The figure is drawn with MOLEKEL [Portmann 2000, Flükiger 2002].

We constructed different hydrated clusters based on $UO_2(CH_3COO)(H_2O)_3$ (Figure 12). They give structural parameters within 15 pm as compared to the experiments when they are optimized in single coordination layer clusters, while the differences do not exceed 4 pm in the two layer two last structures presented in Figure 12. This indicates that further hydrating the first equatorial water molecules improves the model, and adding apical water molecules and hydrating the $O_{acetate}$ atoms still slightly improves the model. The most critical geometric parameters are the U-$O_{acetate}$ and U-O_{water} equatorial first-layer distances. Finally this again illustrates that the coordination number can be deduced from the interpretation of calculated distances.

4.6 MOLECULAR DYNAMICS

It seemed an impossible task to study the role of the second hydration sphere by using static optimizations of realistically large clusters [Bühl Kabrede 2006] before the recent publications of the two sphere cluster method (Section 4.5), which, anyhow, are dependent on the choice of the initial geometry. Theoretically molecular dynamic simulations of the actual solution -namely for infinite systems as modelled with periodic boundary conditions- avoid this problem, providing long enough simulations allow equilibration and exploration of all the relevant geometries. Such long enough times are now reachable by classical molecular dynamics (CℓMD) for hydration, while the residence times of strong ligands are still too long.

4.6.1 CPMD Quantum Dynamic Simulations

The hydration of UO_2^{2+} has been simulated by Carr-Parrinello molecular dynamics (CPMD) [Bühl 2005]. $UO_2(H_2O)_4^{2+}$ or $UO_2(H_2O)_5^{2+}$ was initially placed in a water box (with periodic conditions); no water exchange was observed during the short times (a few pico-seconds) of the simulations. This is not specially surprising, since the expected order of magnitude of the residence time of water in the first coordination sphere of UO_2^{2+} is much longer than the times of the simulations, as pointed out by the authors. Constrained CPMD simulations started with one coordination number and finishing with the other one gave the Helmholtz free energy by integration along the reaction, giving the coordination of 5 as the most stable in liquid water; while the authors concluded that the coordination number is 4 in the gas phase.[40] Such simulations are rather appropriate to obtain the activation barrier between the initial and final configurations, as done by the authors. They also obtained 247 ± 9 pm for the U-OH_2 distance, where the "uncertainty" actually corresponds to fluctuations which are due to thermal agitation, providing that the 4.5 ps of simulation are long enough. In another CPMD study they obtained virtually the same inter-atomic distance for the $UO_2(H_2O)_5^{2+}$ stoichiometry (248 ± 10 pm), and they also report 239 ± 8 pm for $UO_2(H_2O)_4^{2+}$ [Bühl, Kabrede, Diss 2006] in liquid water. According to the authors the largest uncertainty arises from the quantum-chemical method they employed, namely DFT/BLYP. We obtained a shorter distance (242 pm) in our apical two-sphere static model for $UO_2(H_2O)_5^{2+}$ using B3LYP [Siboulet 2006].[5] EXAFS experimental values are 242 pm [Allen 1997] and 241 pm [Neuefeind 2004]. The 5-7 pm overestimation by CPMD simulations might indeed be essentially due to the level of quantum calculation; nevertheless, published CPMD simulations for other cations in liquid water give slightly better agreement with the EXAFS distances (see typically [Spezia 2006]). On the other hand, the U atomic charge is high -about 3- as compared to much of the published CPMD studies of aquo cations. A published constrained CPMD simulation of La^{3+}(aq) gave the correct distance but a coordination number of 8, whereas 9 is accepted in the literature.

The CPMD O_{yl}-H radial distribution function shows a small first peak at about 220 ± 30 pm, but Bühl *et al.* concluded that this is not evidence for apical H_2O H-bonded on the O_{yl}. 220 pm is again longer (by 28 pm) than the 192 pm distance we optimised in our

apical two-sphere static model (Section 4.5.2) [Siboulet 2006]. The existence of this apical bond is still debated (Sections 4.5.2 and 4.6.2). If it exists, it would be anyhow quite weak. It is suggested for interpreting experimental observations [Groenewold 2006].

Constrained CPMD simulations have been used to estimate 40 kJ.mol^{-1} for the Gibb's energy of the hydrolysis reaction of UO_2^{2+} [Bühl, Hendrik 2006].[44] This corresponds to lg^*K_1 = -7.0 ($-pH_{1/2,1}$) for the $^*K_1$ hydrolysis constant, while the measured value is lg^*K_1 = -5.25 ± 0.24 ($\Delta_r{}^*G_1$ = 30 ± 1 kJ.mol^{-1}). This difference of 1.75 log_{10} units is too large compared to the accuracy of experimental solution chemistry, but it corresponds to only 10 kJ.mol^{-1}, which is well within the accuracy of the modelling method.

As a conclusion, these studies indicate that CPMD simulations can give useful results, with some evident limitations (short simulation times, bias of the DFT methods) that must be kept in mind for interpretations. Non-constrained CPMD simulations only explore geometric configurations close to the initial geometry in the same way as static geometry optimisations; but CPMD gives a realistic picture for the geometries and physical parameters that are dominated by dynamics among which activation barriers and the behaviour of the water molecules beyond the quite rigid first coordination sphere.

4.6.2 CℓMD Classical Dynamic Simulations

CℓMD can simulate bigger systems than CPMD, and on longer times. A few CℓMD simulations of UO_2^{2+} complexes in a few solvents and at interfaces have been published [Baaden 2002, Chaumont 2003, Chaumont 2004, Galand 2005, Guilbaud 1996, Hagberg 2005]. CℓMD needs to build and parameterize a force field, and to explicitly calculate the polarization of water by the cation, when it is highly charged -as U in UO_2^{2+} [Clavaguera-Sarrio 2003, Hagberg 2005, Hemmingsen 2000]. This is not necessarily a drawback keeping in mind that published CℓMD models for liquid water give better results -in many respects- than quantum dynamics simulations.

Hagberg *et al.* give much details on their UO_2^{2+}-H_2O pair interaction potential and parameters. They parameterized their potential to reproduce high level quantum calculations for five different series of geometries for $UO_2(H_2O)_2^{2+}$ (Figure 13 a to e). It is not clear whether the apical geometry (Figure 13 f) was used in this parameterisation. They obtained correct geometric results with CℓMD simulations -explicitly calculating the polarisation- for the (240 pm) UO_2^{2+}-OH_2 distance and the (5) equatorial coordination number. They observed some configurations where there exists a weak water hydrogen bond to the uranyl oxygen with length of about 200-250 pm consistent with the 220 ±

[44] The $UO_2(H_2O)_5^{2+}$ + (n-5)H_2O initial system did not include any free H^+ neither HO^-. If this corresponds to pH = 7 the major U(VI) aqueous species would be $UO_2(OH)^+$ with non negligible amounts of $UO_2(OH)_2$(aq) in equilibrium conditions (Figure 2). Similarly, if the $(UO_2(OH)(H_2O)_3^+$ + H_3O^+ + (n-5)H_2O) final system correspond to (1 H_3O^+ for (n-5)H_2O) very acidic condition because [H^+] corresponds to 1 mol.ℓ$^{-1}$, -namely (n-5)/55.5 mol.ℓ$^{-1}$ with the usual n values of CPMD simulations- the major U(VI) species would be UO_2^{2+} in equilibrium conditions, actually the initial species: there are about 7 pH unit (40 kJ.mol^{-1} at 25°C) difference between the initial and final aqueous solutions.

30 pm observed by CPMD simulations (Section 4.6.1). They concluded there is no apical water. The two molecular dynamics simulations used much different theoretical approaches: CℓMD using a model parameterized with high level ab initio calculations and CPMD consisting of quantum calculations but of (BLYP DFT) less sophisticated level of quantum calculation. Our static two sphere cluster calculations gave a (192 pm) shorter apical distance (Section 4.5.2). The 30 pm shorter static distance (as compared to the dynamics mean distance) is not exceptional for such long weak bonds in liquid water, since the temperature effects are not included in the static calculations. Furthermore, deciding whether the 220-225 pm O-(HOH)apical mean distance is -or not- a hydrogen bond can very well be a matter of appreciation. This is still an open question.

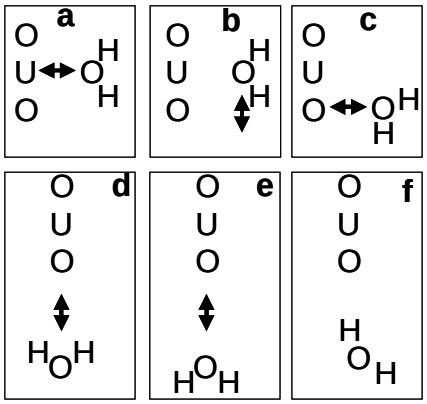

Figure 13. Geometries to fit the interaction potential of UO_2^{2+} -OH_2

as used by Hagberg *et al.* (a, b, c, d and e): The arrows show the geometric parameters that are varied [Hagberg 2005]. Apical H_2O (f) is also shown.

The way force fields had been obtained have recently been discussed for La^{3+} -and other (Ln^{3+}) lanthanide tri-cations- in liquid water [Duvail Souaille 2007]. For these ions it appeared from the literature that the best results were not obtained by trying to reproduce -in the pair-interaction potential (of the force field)- quantum energies of the system containing the (1 La^{3+} + 1 H_2O) pair of species. Better results were obtained by using (typically 1 La^{3+} + 8 H_2O) bigger model clusters and trial simulations in the parameterization process. This suggests that -at least- some of the parameters of such a cation-water force field can be only phenomenological rather than purely atomic, as they also are for popular models of liquid water, where different sets of parameters are often used for gas and liquid water. Nevertheless, the La^{3+} / H_2O pair interaction potential was extended to the other Ln^{3+} cations without new fittings of the parameters: their values were changed based on published ionic radii among the Ln^{3+} series [Duvail 2008].

It is generally believed that such approach can also be extrapolated to the (An^{3+}) actinide tri-cations, namely the difference in the ionic radii are supposed to be sufficient to explain the small differences in the chemistries of the cations of the f-block elements with the same charge. These ions are indeed chemical analogues as typically reflected in the difficulty to separate the two series -namely long lived Am^{3+} and Cm^{3+} activation products from light Ln^{3+} fission products- in the industrial reprocessing of nuclear spent

fuels. On the other hand small differences are expected between the two series.

A difficulty of CℓMD -as compared to quantum methods- is that it is needed to evidence the relevant physical phenomenons to include them in the model with the known or fitted parameters. Unfortunately, the physical meanings of the parameters can be questionable, when curve fitting is used.

$Ln(H_2O)_{i-1}^{3+}/Ln(H_2O)_i^{3+}$ water exchanges were observed by CℓMD simulations for i = 7 to 10. It was interpreted with the same methodologies as experimental solution chemistry: it gives K_i,[45] the constant of the equilibrium -or equivalently $\Delta_r G_i$- for each simulation providing such thermodynamics interpretation is relevant.[46] A classical van't Hoff interpretation accounted for the temperature influence studied by performing different simulations with different target temperatures. This gave the $\Delta_r H_i$ enthalpy and $\Delta_r S_i$ entropy contributions to the $\Delta_r G_i$ values [Duvail Spezia 2007].[47] Obtaining the van't Hoff interpretation gives confidence in the CℓMD simulations. This thermodynamic interpretation also gives the changes with temperature of the contribution of the bulk water.[48] All these terms correspond to quite small energy changes as compared to the total energy of the system. This is possible, since $\Delta_r G$, $\Delta_r H$ and $\Delta_r S$ are obtained by population analysis -namely from K- not by calculating energy terms. This is a similar procedure as used in experimental solution chemistry, where the equilibrium constants are usually obtained by changing the proportions of reactants and products -typically by chemical titrations in controlled buffered conditions- and measuring physical data that are determined by the concentrations of reactants or (and) products. Such approach can be used for any chemical equilibrium providing the reaction is observed and the system equilibrated. This was possible for hydration because the residence time of water was smaller than the times of the CℓMD simulations, and because the molecular model at the base of the CℓMD simulations allows exchanged of water molecules. This last feature will still stand for complexes in which the intra-molecular interactions can be described by electrostatics, polarization and small contributions of charge transfer. When the charge transfer is more important, quantum descriptions are needed. In this case bonds are stronger; consequently residence times of the ligands are longer, while only shorter times are reachable (by CPMD as compared to CℓMD): the population analysis method

[45] The constant of Equilibrium $Ln(H_2O)_{i-1}^{3+} + H_2O \leftrightarrows Ln(H_2O)_i^{3+}$ is $K_i = \frac{[Ln(H_2O)_i^{3+}]}{[Ln(H_2O)_{i-1}^{3+}]} = \frac{n_i}{n_{i-1}}$ where n_i is the number of $Ln(H_2O)_i^{3+}$ configurations, since P and T can be considered to be constant during a given simulation.[46] $\Delta_r G_i = -R\,T\,\ln K_i$.[48]

[46] Equilibrium constant are (constant) for constant temperature (T) and pressure (P), while molecular dynamics simulations are usually performed in the NVE or NVT ensemble. However, after equilibration calculated T values are within usual fluctuations during NVE simulations. Similarly, the variations of P during the simulations usually have negligible influence on log K.

[47] The van't Hoff approximation is $R \ln K(T) = R \ln K(T^\circ) - \Delta_r H(T^\circ)\,(1/T - 1/T^\circ)$. It assumes negligible influence of T on $\Delta_r H$, or equivalently on $\Delta_r S$, or equivalently $\Delta_r C_p = 0$. The slope of the (R ln K *v.* 1/T) van't Hoff plot gives $-\Delta_r H$, and the intercept gives $\Delta_r S = \Delta_r H / T^\circ + R \ln K(T^\circ)$.

[48] Assuming that the simulation correspond to standard conditions (namely infinite dilution, see Section 3.4.1.3), $\Delta_r G_i = \Delta_r G_i^0 = \Delta_f G_i^0 - \Delta_f G_{i-1}^0 - \Delta_f G_{H_2O(\ell)}^0$ where $\Delta_f G_{H_2O(\ell)}^0$ is known experimentally at each temperature. This term is implicitly included in K at 25°C when using the $|H_2O| = 1$ convention; however $\Delta_f G_{H_2O(\ell)}^0$ depends on T.

cannot be used. Alternatively constrained CPMD simulations have been used but the accuracy is probably less than for experimental measurements (4.6.1).

4.7 THE STABILITIES OF $An(OH)_4^{(Z-4)+}$ SPECIES IN SOLUTION: AN UN-RESOLVED QUESTION

We have seen above that $U(OH)_4(aq)$ is unexpectedly, even anomalously, stable in aqueous solution, as its predominance domain is large (Figure 2, Figure 3). A few aqueous hydroxides of other cations also have relatively large predominance domains. Is this due to their charge, to particular geometries of their hydrations or to the formation of unsuspected isomers? Namely, all the U(Z) (Z is the oxidation number of U) oxo-hydroxo-ions of same charge are isomers when equilibrated with liquid water: changing the number of (O^{2-}) oxo and (HO^-) hydroxo ligands corresponds to hydrolysis -or conversely to protonation- reactions; but for solution chemistry all the $UO_i(OH)_{Z-2i-z}^{z+}$ species are isomers as typically obtained by simultaneous protonation of an O_{yl} and hydrolysis in the equatorial plane:[13] $U(OH)_4(aq)$, $UO(OH)_2(aq)$ and $UO_2(aq)$ are isomer, but the solubility of the neutral U(IV) aqueous hydroxide is too low to allow physical measurements that would give direct indications on its geometry, typically whether $UO_2(aq)$ would be stable, or whether $U(OH)_4(aq)$ has an especially stabilizing hydration geometry among many other possible explanations. As far as we are aware, no convincing explanation is available at present for this phenomenon. The geometrical parameters computed for gas-phase $U(OH)_4$ with DFT (B3LYP) are in no way exceptional, as shown in Table 1. In the gas phase, the molecule has C_{2v} symmetry (almost tetrahedral), but the nature of this species in solution is not yet established. What will the coordination number of uranium be? We do not know of any published experimental data (EXAFS, vibrational spectroscopy, …) that could shed light this question. The modelling of $U(OH)_4$ in aqueous solution is not a trivial task, since many different types of structure with different coordination numbers and hydrogen-bonded networks will need to be considered. This is a task for the future.

Table 1. Geometric data for $An(OH)_4^{(z-4)+}$.

z	6		5		4	
Th-O (pm)					216.7	
Th-H (pm)					96.4	
Th-O-H (°)					180	
Pa-O (pm)			204.5		212.2	
Pa-H (pm)			97.2		96.5	
Pa-O-H (°)			180		180	
U-O (pm)	195.4	196.0	200.9	203.2	210.7	211.1
O-H (pm)	99.2	98.7	97.2	97.4	96.4	96.5
O-U-O (°)	165	103	104	141	107	108
U-O-H (°)	162	178	175	165	177	172

CONCLUSION

A first application of molecular modelling is building geometries of molecules. This, together with EXAFS experimental data, can be used as a speciation tools for solution chemistry. Molecular modelling can reproduce the distance between uranium and the donor atoms of the coordinated ligands surprisingly well in aqueous uranyl complexes. This is exemplified here for model UO_2^{2+} hydrated clusters and a few complexes. The correct distances can be obtained by optimizing the geometries of two-hydration-layer model clusters with DFT (B3LYP) quantum calculations. To our knowledge, this two-sphere method was recently published and first used for UO_2^{2+}, whose linear geometry certainly eases the geometric construction of the coordinating clusters. Such geometry results can be compared to EXAFS experimental data, to help the interpretation of experiments, to validate quantum calculations, or even to find the most stable geometry when isomers have similar energies -*i.e.* within 10 or a few tens of kJ.mol^{-1}-. This have been exemplified in a few examples for complexes in which the U-ligand equatorial bond lengths are also surprisingly well reproduced when optimizing -by DFT (B3LYP) quantum calculations- the geometries of clusters made of a complex with up to two hydration layers of the central cation. This method allows to include enough water molecules in the clusters, but it has its limits: typically the DFT quantum method is known to have some limitations for modelling liquid water. Static geometry optimisations and associated harmonic vibration post-treatments often poorly reproduce temperature effects in aqueous solutions. Another main difficulty can be the choice and construction of the correct geometry, since geometry optimisations are often dependent on the initial geometry guess, when the potential energy surface has many different minima. Nevertheless, at least for a few examples the method is accurate enough to help interpreting experimental geometrical results. Simulating the bulk solution with a dielectric continuum gives similar results using only one hydration layer; however careful examination of the explicit second hydration layer pointed out that apical water might have some importance, this is still an open question that has also been investigated by CPMD and CℓMD simulations.

A second application of molecular modelling is, of course, describing the electronic configurations of the chemical systems, especially covalent bonds and atomic charges despite they are not direct quantum physical parameters, but rather chemical parameters extracted from quantum calculation results. They can be used to check and better understand qualitative interpretations commonly used by chemists, and even to open routes for finding new binding modes in eventually new molecules. Quantum calculations indicate that the great stability of UO_2^{2+} is due to the two U≡O_{yl} triple covalent bonds. In most cases the equatorial ligands have little influences on these covalent bonds. The f-character of the AnO_2^{z-4} bonding increases across the $^{90}ThO_2$ < $^{91}PaO_2^+$ < $^{92}UO_2^{2+}$ isolelectronic series. UO_2^{2+} is the first very stable actinyl, while protactinyl PaO_2^+ is not much stable in aqueous solution, where (stable) $PaOOH^{2+}$ is the only protonated AnO_2^{z-4}. This explains that Pa(V) is not a chemical analogue of the other

actinides(V), while all the other f-elements are chemical analogues when in the same oxidation state. A greater variety of geometries are found for Pa(V) as compared to iso-electronic U(VI), certainly corresponding to a greater variety of electronic configurations for Pa(V) as compared to U(VI). This certainly opens the field to further quantum chemical studies of Pa(V) and other f-elements, first studying the details of the electronic configurations on small Pa(V) covalent (ionic) molecules and iso-electronic U(VI) ones, typically including tetrahedral $Pa(OH)_4^+$, which have recently been proposed to be quite stable [Siboulet 2008]. Indeed tetrahedral UO_4^{2-} has also been calculated despite it is readily hydrated by any trace of water, which should destroy the tetrahedral skeleton (Figure 9).

It is generally believed that the f-block elements form hard cations. This indeed qualitatively explains the stabilities of the complexes as reflected by equilibrium constants, but quantum calculations can be interpreted with non negligible charge transfer between UO_2^{2+} and its HO^- equatorial ligands: hardness should be understood as correlation between electrostatics and chemical observations, but not as formation of purely electrostatic bonds.

Equilibrium constants represent small ($\Delta_r G$) energy changes as compared to the total energy of the system. Nevertheless, a given equilibrium constant can very well be measured with good accuracy. This is simply obtained by shifting the equilibrium probing the concentrations of the reactants and products of interest and controlling the auxiliary chemical species and conditions: namely very small energy changes are obtained with good accuracy without measuring or explicitly using the total energy of the system. This could be used with molecular modelling; indeed the same methodology was used to interpret molecular dynamics simulations of the hydration of La^{3+} in aqueous solutions, namely K_i (hence $\Delta_r G_i$) values were extracted from population analysis of the different $La(H_2O)_i^{3+}$ species -hence without using the total energy of the system. The ($\Delta_r H_i$) enthalpy changes were further obtained from the influence of the temperature on the ($\Delta_r G_i$) Gibbs energy changes (van't Hoff plot). Again this gave ($\Delta_r G_i$ and $\Delta_r H_i$) energy changes that represent only a very small part of the total energy on the systems during the simulations. Theoretically, this method can be extended from hydration to complexation equilibria providing equilibration can be achieved within the time of the simulations. Unfortunately, this requirement is not fulfilled for complexation, because the residence time of the ligands are too long as compared to the affordable times of molecular dynamics simulations. Alternatively, it has been proposed to perform constrained molecular dynamics.

A regular increase of binding energies is usually observed when adding one by one a ligand to a cation, in the gas phase. Does this necessarily correspond to regular increase of the successive formation constants for the aqueous species? This cannot be predicted, because the energies of hydration are more important than the ($\Delta_r G$) Gibbs energy of the reactions between aqueous species. Typically, the hydration geometry of tetrahedral $U(OH)_4$ is not well known.

REFERENCES

Allen, P. G.; Bucher, J. J.; Shuh, D. K.; Edelstein, N. M.; Reich, T. *Inorg. Chem.* 1997, *36*, 4676-4683.

Baaden, M.; Schurhammer, R.; Wipff, G. *J. Phys.Chem. B* 2002, *106*, 434-441.

E. J. Baerends, J. Autschbach, A. Bérces, F. M. Bickelhaupt, C. Bo, P. M. Boerrigter, L. Cavallo, D. P. Chong, L. Deng, R. M. Dickson, D. E. Ellis, M. van Faassen, L. Fan, T. H. Fischer, C. Fonseca Guerra, S. J. A. van Gisbergen, J. A. Groeneveld, O. V. Gritsenko, M. Grüning, F. E. Harris, P. van den Hoeck, C. R. Jacob, H. Jacobsen, L. Jensen, G. van Kessel, F. Koostra, E. van Lenthe, D. A. McCormack, A. Michalak, J. Neugebauer, V. P. Osinga, S. Patchkovskii, P. H. T. Philipsen, D. Post, C. C. Pye, W. Ravenek, P. Ros, P. R. T. Schipper, G. Schreckenbach, J. G. Snijders, M. Solà, M. Swart, D. Swerhone, G. te Velde, P. Vernooijs, L. Versluis, L. Visscher, O. Visser, F. Wang, T. A. Weselowski, E. van Wezenbeek, G. Wiesenekker, S. K. Wolff, T. K. Woo, A. L. Yakovlev and T. Ziegler, 2006.

Becke, A. D. *J. Chem. Phys.*, 1993, *98*, 5468-5652.

Bühl, M.; Diss, R.; Wipff, G. *J. Am. Chem. Soc.* 2005, *127*, 13506-13507.

Bühl, M.; Hendrik K. *ChemPhysChem*. 2006, *7*, 2290-2293.

Bühl, M.; Kabrede H. *Inorg. Chem.* 2006, *45*, 3834-3836.

Bühl, M.; Kabrede H.; Diss, R.; Wipff, G. *J. Am. Chem. Soc.* 2006, 128, 6357-6368.

Cao, Z.; Balasubramanian, K. *J. Chem. Phys.* 2005, *123*, 114309.

Capdevila, H.; Vitorge P. *J. Radioanal. and Nuclear Chem.* Articles, 1990, *143*, 403-414.

Chaumont, A.; Engler, E.; Wipff, G. *Inorg. Chem.* 2003, *42*, 5348-5356.

Chaumont, A.; Wipff, G. *Chem.s Eur. J.* 2004, *10*, 3919-3930.

Clavaguéra-Sarrio, C.; Brenner, V.; Hoyau, S.; Marsden, C. J.; Millié, P.; Dognon, J.-P. *J. Phys. Chem. B.* 2003, *107*, 3051-3060.

Conradson, S.; Manara, D.; Wastin, F.; Clark, D.; Lander, G.; Morales, L.; Rebizant, J.; Rondinella, V. *Inorg. Chem.* 2004, *43*, 6922-6935.

Cramer, C. J.; Truhlar, D. G. *Chem. Rev.* 1999, *99*, 2161-200.

Denis, J.; Michard, G. *Bull. Minéral.* 1983, *106*, 306-309.

Duvail, M.; *Thèse* 2007, Université d'Orsay, Orsay, France.

Duvail, M.; Souaille, M.; Spezia, R.; Cartailler, T.; Vitorge, P. *J. Chem. Phys.* 2007, *127*, 034503-034511.

Duvail, M.; Spezia, R.; Cartailler, T.; Vitorge, P. *Chem. Phys. Letters* 448, 2007, *1*, 41-45.

Duvail, M.; Spezia, R.; Vitorge, P. *ChemPhysChem.* 2008, *9*, 693-696.

Ferri, D.; Salvatore, F.; Vasca, E.; Glaser, J.; Grenthe, I. *Acta Chem. Scand.* 1993, *47*, 855-861.

Flükiger, Lüthi, H. P.; Portmann, S.; Weber, S. J. *MOLEKEL 4.2 P.* 2002, Swiss Center for Scientific Computing, Manno (Switzerland).

Fonseca Guerra, C.; Snijders, J. G.; te Velde, G.; Baerends, E. J.; *Theor. Chem. Accounts*, 1998, *99*, 931.

Fuchs, M. S. K.; Shor, A. M.; Rosch, N. *International J. Quant. Chem.* 2002, *86*, 487-501.

Galand, N.; Wipff, G. *J. Phys. Chem. B* 2005, *109*, 277-287.

Gaussian 03, Revision C.02, Frisch, M. J.; Trucks, G. W.; Schlegel, H. B.; Scuseria, G. E.; Robb, M. A.; Cheeseman, J. R.; Montgomery, Jr., J. A.; Vreven, T.; Kudin, K. N.; Burant, J. C.; Millam, J. M.; Iyengar, S. S.; Tomasi, J.; Barone, V.; Mennucci, B.; Cossi, M.; Scalmani, G.; Rega, N.; Petersson, G. A.; Nakatsuji, H.; Hada, M.; Ehara, M.; Toyota, K.; Fukuda, R.; Hasegawa, J.; Ishida, M.; Nakajima, T.; Honda, Y.; Kitao, O.; Nakai, H.; Klene, M.; Li, X.; Knox, J. E.; Hratchian, H. P.; Cross, J. B.; Bakken, V.; Adamo, C.; Jaramillo, J.; Gomperts, R.; Stratmann, R. E.; Yazyev, O.; Austin, A. J.; Cammi, R.; Pomelli, C.; Ochterski, J. W.; Ayala, P. Y.; Morokuma, K.; Voth, G. A.; Salvador, P.; Dannenberg, J. J.; Zakrzewski, V. G.; Dapprich, S.; Daniels, A. D.; Strain, M. C.; Farkas, O.; Malick, D. K.; Rabuck, A. D.; Raghavachari, K.; Foresman, J. B.; Ortiz, J. V.; Cui, Q.; Baboul, A. G.; Clifford, S.; Cioslowski, J.; Stefanov, B. B.; Liu, G.; Liashenko, A.; Piskorz, P.; Komaromi, I.; Martin, R. L.; Fox, D. J.; Keith, T.; Al-Laham, M. A.; Peng, C. Y.; Nanayakkara, A.; Challacombe, M.; Gill, P. M. W.; Johnson, B.; Chen, W.; Wong, M. W.; Gonzalez, C.; and Pople, J. A.; Gaussian, Inc., Wallingford CT, 2004.

Glendening, E. D.; Reed, A. E.; Carpenter, J. E.; Weinhold, F. *NBO Version 3.1*, 1998.

Grenthe, I.; Fuger, J.; Konings, R. J. M.; Lemire, R.; Muller, A. B.; Nguyen-Trung, C.; Wanner, H.; *Chemical Thermodynamics of Uranium* NEA OECD Paris, FRANCE, and Elsevier Amsterdam NORTH-HOLLAND, 1992; http://www.nea.fr/html/dbtdb/pubs/uranium.pdf.

Gresham, G. L.; Gianotto, K.; Harrington, P.; Cao, L.; Scott, J. R.; Olson, J. E.; Appelhans, A. E.; Van Stipdonk, M. J.; Groenewold, G.S. *J. Phys. Chem. A* 2003, *107*, 8530-8538.

Groenewold, G.; Gianotto, A. K.; Cossel, K. C.; Van Stipdonk, M. J.; Moore, D. T.; Polfer, N.; Oomens, J.; de Jong, W. A.; Visscher, L.; *J. Am. Chem. Soc.* 2006, *128*, 4802 -4813.

Guilbaud, P.; Wipff, G. *J. Phys. Chem.* 1993, *97*, 5685-5692.

Guilbaud, P.; Wipff, G. *THEOCHEM* 1996, *366*, 55-63.

Gutowski, K. E.; Dixon, D.A.; *J. Phys. Chem. A*, 2006, *110*, 8840-8856.

Hagberg, D.; Karlström, G.; Roos, B. O.; Gagliardi, L. *J. A. C. S.* 2005, *127*, 14250-14256.

Hay, P. J.; Martin, R. L.; Schreckenbach, G. *J. Phys. Chem. A* 2000, *104*, 6259-6270.

Hemmingsen, L.; Amara, P.; Ansoborlo, E.; Field, M. J. *J. Phys. Chem. A* 2000, *104*, 4095-4101.

Hennig, C.; Schmeide, K.; Brendler, V.; Moll, H.; Tsushima, S.; Scheinost, A. C. *Inorg. Chem.* 2007, *46*, 5882–5892.

Humphrey, W.; Dalke, A.; Schulten, K. *J. Molec. Graphics* 1996, *14.1*, 33-38. VMD, http://www.ks.uiuc.edu/Research/vmd/.

Ikeda, A.; Hennig, C.; Rossberg, A.; Tsushima, S.; Scheinost, A. C.; Bernhard, G. *Anal. Chem.* 2008, *80*, 1102-1110.

Ismail, N.; Heully J.-L.; Saue, T.; Daudey, J.-P.; Marsden, C. J. *Chem. Phys. Letters* 1999; *300*, 296-302.

Jiang, J.; Rao, L.; Di Bernardo, P.; Zanonato, P. L.; Bismondo, A. J. *Chem. Soc., Dalton*

Trans. 2002, *8*, 1832-1838.
Lemire, R.; Fuger, J.; Nitsche, H.; Rand, M.; Spahiu, K.; Sullivan, J.; Ullman, W.; Vitorge. P. *Chemical Thermodynamics of Neptunium and Plutonium*. OECD Paris, FRANCE, and Amsterdam NORTH-HOLLAND, Elsevier, 2001.
Lippmann, F. *N. Jb. Mineral. Abh.* 1977, *130*, 243-263.
Lippmann F. *N. Jb. Mineral. Abh.* 1980, *139*, 1-25.
Michard, G. *Bull. Minéral.* 1986, *109*, 239-251.
Michard, G. *Initial edition of [Michard 2002]*, 1989.
Michard, G. *Chimie des eaux naturelles : principes de géochimie des eaux*. Publisud Paris, FRANCE, 2002.
Moll, H.; Geipel, G.; Reich, T.; Bernhard, G.; Fanghänel, T.; Grenthe, I. *Radiochim. Acta* 2003, *91*, 11-20.
Moskaleva, L. V.; Kruger, S.; Sporl, A.; Rosch N. *Inorg. Chem.* 2004, *43*, 4080-90.
Neuefeind, J.; Soderholm, L.; Skanthakumar, S. *J. Phys. Chem. A* 2004, 108, 2733-2739.
Neuefeind, J.; Skanthakumar, S.; Soderholm, L. *Inorg. Chem.* 2004, *43*, 2422–2426.
Nguyen-Trung, C.; G.M. Begun, D.A. Palmer, *Inorg. Chem.* 1992, *31*, 5280-5287.
Portmann, S.; Lüthi, H. P.; *Chimia* 2000, *54*, 766-770.
Rai1, D.; Hess1, N. J.; Yui2, M.; Felmy1 A. R.; Moore D. A. *Radiochim. Acta* 2004, *92*, 527–535.
Reed, A. E.; Curtiss, L. A.; Weinhold, F.; Aas, W. *Chem. Rev.* 1988, *88*, 899.
Rotzinger, F. P. *Chem.sEur. J.* 2007, *13*, 800-811.
Schaftenaar, G. 1991, Molden, http://www.cmbi.kun.nl/~schaft/molden/molden.html.
Schlosser, F.; Kru1ger, S.; Rö1sch, N. *Inorg. Chem.* 2006, *45*, 1480-1490.
Shamov, G. A.; Schreckenbach, G. *J. Phys. Chem. A.*, 2005, *109*, 10961-10974.
Siboulet, B.; Marsden, C.J.; Vitorge, P. *Chem. Phys.* 2006, *326*, 289-296.
Siboulet, B.; Marsden, C.J.; Vitorge, P. *VHM–2006*, http://www-ist.cea.fr/publicea/exl-doc/200600002604_s1.pdf.
Siboulet, B.; Marsden, C.J.; Vitorge, P. *New J. Chem.* 2008, *32*, 2080-2094.
Spencer, S.; Gagliardi, L.; Handy, N. C.; Ioannou, A. G.; Skylaris, C.-K.; Willets, A.; Simper, A. M. J. *Phys. Chem. A* 1999, *103*, 1831-1837.
Spezia, R.; Duvail, M.; Vitorge, P.; Cartailler, T.; Tortajada, J.; Chillemi, G.; D'Angelo, P.; Gaigeot, M.-P. *J. Phys. Chem. A*, 2006; *110*, 13081 – 13088.
Stokes, R. In *Activity coefficients in electrolyte solutions.* Pitzer K. Ed.; Publisher: CRC press:, Boca Raton, FL, 1991, pp. 1-28
Tomasi, J.; Persico, M. *Chem. Rev.* 1994, *94*, 2027-2094.
Tomasi, J.; Cammi, R.; Mennucci, B.; Cappelli, C.; Corni, S. *Phys. Chem. Chem. Phys.* 2002, *4*, 5697-5712.
Toraishi, T.; Tsuneda, T.; Tanaka, S. *J. Phys. Chem. A* 2006, *110*, 13303-13309.
te Velde, G.; Bickelhaupt, F. M.; van Gisbergen, S. J. A.; Fonseca Guerra, C.; Baerends, E. J.; Snijders, J. G.; Ziegler, T. *J. Comput. Chem.* 2001, *22*, 931.
Vallet, V.; Grenthe, I. *C. R. Chim.* 2007, *10*, 905–915.
Vallet, V.; Wahlgren, U.; Schimmelpfennig, B.; Moll, H.; Szabó, Z.; Grenthe, I. *Inorg. Chem.* 2001, *40*, 3516-3525.

Vallet, V.; Wahlgren, U.; Schimmelpfennig, B.; Szabó , Z.; Grenthe, I. *J. Am. Chem. Soc.* 2001, *123*, 11999-12008.
Vercouter, T.; Vitorge, P.; Amekraz, B.; Moulin, C. *Inorg. Chem.* 2008, *47*, 2180-2189.
Vitorge, P.; Capdevila, H.; Maillard, S.; Fauré, M.-H.; Vercouter, T. *J. Nuclear Sc. Techno.* 2002 *Supplement 3*, 713-716.
Vitorge, P.; Capdevila, H. *Radiochim. Acta* 2003, *91*, 623–631.
Vitorge, P.; Phrommavanh, V.; Siboulet, B.; You D.; Vercouter, T.; Descostes, M.; Marsden, C.J.; Beaucaire, C.; Gaudet. J.-P. *Comptes Rendus Chim. Special Issue "Nuclear Energy and Radiochem."* 2007, *10*, 978-993.
Vitorge, P. (2008) *Law of Mass Action for co-Precipitation.* Saclay, France: CEA-R-6193.
Wahlgren, U.; Moll, H.; Grenthe, I.; Schimmelpfennig, B.; Maron, L.; Vallet, V.; Gropen, O. J. *Phys. Chem. A* 1999, *103*, 8257-8264.